FINAL REPORT

MECHANICAL PROPERTIES AND THE ELECTRONIC STRUCTURE OF TRANSITION OF METAL ALLOYS

GRANT #NSG-3001

by

Dr. R.J. Arsenault
Dr. H.D. Drew

Submitted to

NASA, Lewis Research Center
Cleveland, Ohio

UNIVERSITY OF MARYLAND
DEPARTMENT OF PHYSICS AND ASTRONOMY
COLLEGE PARK, MARYLAND

FINAL REPORT

MECHANICAL PROPERTIES AND THE ELECTRONIC STRUCTURE OF TRANSITION OF METAL ALLOYS

GRANT #NSG-3001

Submitted to

NASA, Lewis Research Center
Cleveland, Ohio

UNIVERSITY OF MARYLAND
Department of Physics and Astronomy
College Park, Maryland
20742

I. Introduction

This interdiscipline research program was undertaken in an effort to investigate the relationship between the mechanical strength of Mo based alloys with their electronic structure. That such a relationship may exist for these alloys was suggested by the work of Stephens and Witzke.[1] The program was to consist of a collaborative effort in which Prof. Drew would study the electronic properties of these alloys through optical studies and Prof. Arsenault would examine the classical solid solution strengthening mechanisms based on size and molecular differences to determine if these mechanisms could explain the hardness data. It was hoped that these efforts would lead to a theory of the mechanical strength of this class of alloys. The program was not successful to this extent. However, the optical data does suggest a large potential scattering effect in the alloys that increases the more the solute valency differs from that of the host. This potential scattering implies a d→s charge transfer which should have a significant effect on the bonding of the solute atoms. A more detailed understanding of the mechanical strength of these alloys will have to await more theoretical analysis of these results.

In the next section we describe the optical experiments. Then in Section III the work on the classical solid solution theory is discussed.

II. Optical Experiments

The best understood disordered transition metal alloys are those with noble metal hosts and low concentrations of Ni or Pd.[2,3] In these alloys the impurity d levels fall above the host d bands, and lie in the nearly free electron s-p bands with which they weakly mix to form virtually bound states. The optical properties of these alloys are particularly simple as the absorption associated with the impurity d levels falls at lower frequencies than the interband edge, and is therefore superimposed on a smooth structureless background. Optical studies of CuNi,[4,5,6] AuNi,[5,7] CuPd,[8] AgPd[8-12] and AuPd[8] have proven very fruitful. Also, photoemission studies on these alloys display the impurity density of states clearly separated from the host d bands.[13]

More generally the impurity d levels fall within the host d bands in transition metal alloys.[2] In this case the impurity density of states is expected to have a larger energy width and a more complex spectrum. The theory of the electronic structure of these alloys is much more complex so that our understanding of them is much poorer. Unfortunately the experiments are also more difficult to interpret in this case since the host d bands also change upon alloying, and it is difficult to separate these changes from those due to the added impurity levels (assuming such a separation is justified). Consequently there have been few measurements and still fewer interpretation of optical or photoemission spectra for these alloys, even though these are just the alloys of the most technological interest.

In this work we present a study of the optical and electronic properties of alloys of the 5d transitional elements with Mo. In particular we have studied the MoRe, MoOs and MoPt alloy systems for low 5d element

concentrations. These alloys present two kinds of difficulties to optical studies. The first is that their electronic structure is complex. The second difficulty concerns the preparation of high quality samples of these refractory alloys suitable for optical studies. We solved this second problem by preparing film by the co-evaporation of the two constituents of the alloy with separate e-gun sources. The first problem has prevented a complete understanding of the electronic structure of the alloys but this work has provided important new data which should provide significant clues to the determination of the electronic structure of these alloys.

A. EXPERIMENTAL

The samples were prepared by simultaneous vacuum evaporation of the two constituents onto polished fused quartz substrates, 1 mm thick by 25.4 mm diam. Two substrates were mounted in the evaporation chamber in the geometry shown in Fig. 1, so that a shield placed between the two sources prevented the solute vapor from falling onto the pure substrate while permitting the Mo vapor to fall on both. The deposition rates were typically 50 Å/sec (monitored by a quartz oscillator), and the total thickness was typically 3000 Å. The solute was evaporated with a Varian 2-kilowatt electron-beam evaporation source, while Mo was evaporated with a 6-KW electron-beam evaporator. The evaporation chamber was evacuated by a conventional oil diffusion pump with liquid nitrogen cold trap. During film deposition the pressure was about 5×10^{-6} Torr and during the subsequent annealing (400° C for 15 Min) it went down to about 5×10^{-7} Torr. Lower annealing temperatures were unsatisfactory because the reflectivity results were then found to change for several days, as the samples continued to anneal at room temperature. The 400° C annealing temperature produced stable results. The solute concentrations were determined from

dc resistivity ratios of the samples between room temperature and 4° K using the resistivity data in the literature and calibrated corrections by chemical analysis of several of our films. Our concentration determination was accurate to about 10% relative.

Reflectivity measurements were made with a single beam differential reflectometer similar to that described by Beaglehole.[14] Both pure and alloy samples were mounted on a rotating holder so that light was reflected alternately from a pure molybdenum and an alloy sample. The quantity $\alpha \equiv (R_{pure} - R_{alloy})/(R_{pure} + R_{alloy})$ was recorded continuously as a function of photon wavelength.

A typical spectrum of α vs. ω is shown in Fig. 2. α was measured to one part in 10^4 in the visible, and the precision fell off to one part in 10^3 in the infrared (below 0.6 eV) and in the ultraviolet (above 5 eV). Only pure and alloy samples prepared at the same time were compared with one another in order to reduce the reflectivity differences due to variations of vacuum evaporation conditions and the effects of 'aging' after exposure to air. The reflectivities of our pure Mo films were measured separately using a Perkin-Elmer Model 350 spectrophotometer with a specular reflectance accessory. We found agreement to within a few percent over the measured spectral range with the published results on bulk samples.[15,16]

The complex conductivity function $\sigma = \sigma_1 + i\sigma_2$ of the sample was obtained through a Kramers-Kronig analysis of the reflectivity data. σ_{pure} and σ_{alloy} were determined separately from R_{pure} and $R_{alloy} = R_{pure}\left(\frac{1-\alpha}{1+\alpha}\right)$. The results were then presented in terms of the differential conductivity $\nabla\sigma_1 = \sigma_1^{alloy} - \sigma_1^{pure}$. In order to perform the Kramers-Kronig analysis it was necessary to extrapolate the reflectivity data outside the measured spectral range. For the low-energy extrapolation we modeled the complex dielectric function $\varepsilon = 1 + \frac{4\pi i\sigma}{\omega}$ as the sum of a Drude term for the

conduction electron response and a simple Lorentzian oscillator term to account in an approximate way for the interband absorption. The oscillator frequency was located well above the low frequency cut off, ω_ℓ, at 0.5 eV. Thus for the low-energy extrapolation, we have

$$\varepsilon(\omega) \simeq 1 - \frac{\omega_p^2}{\omega(\omega+i/\tau)} + \frac{f}{\omega_o^2 - \omega^2 - i\Gamma\omega} \quad , \omega < \omega_\ell \quad . \tag{1}$$

For the Drude term we used the plasma frequency (ω_p = 8.4 eV) given for pure Mo,[15] and assumed that it was unchanged for the alloy. The life-time τ was taken as the zero-frequency value determined from the dc resistivity. The three parameters in the Lorentzian oscillator term were then determined by a least squares fit to the reflectivity data near the low frequency cut off at $\hbar\omega_\ell$ = 0.5 eV. This procedure is found to provide a physically consistent low-energy extrapolation. However, the results for $\Delta\sigma$ are not very sensitive to this extrapolation, even if much simpler procedures are used, except very near the cut-off frequency.

We extrapolated our reflectivity data for pure Mo to higher energy (ω > 6.8 eV) so that the Kramers-Kronig inverted optical conductivity, $\sigma_1(\omega) = \omega\,\varepsilon_2(\omega)/4\pi$, matched the data of Koelling et. al.[16] around 2 eV where their results are most reliable. $\sigma_1(\omega)$ obtained in this manner for our pure Mo film is shown in Fig. 3. For alloy samples we modified the extrapolation in order to satisfy the differential conductivity sum rule

$$\Delta n = \frac{2m}{\pi e^2} \int_0^{\omega_s} \Delta\sigma_1(\omega')d\omega' \quad , \tag{2}$$

where Δn is the difference of the density of valence electrons between pure Mo and the alloys. The high frequency cut-off ω_s in Eq. (2) was taken to

be the frequency for the saturation of the sum rule for valence electrons in the pure system. We chose ω_s to be 30 eV, corresponding to the experimental result for pure Au.[17] Although the magnitude of $\sigma_1(\omega)$ within the data range is in general strongly dependent on the choice of the high energy extrapolation function, the results for $\Delta\sigma_1 = \sigma_1^{alloy} - \sigma_1^{pure}$ obtained this way were practically insensitive to the extrapolation functions.

B. DISCUSSION

The results for representative MoRe, MoOs and MoPt films are shown in Figures 4, 5 and 6. We will be discussing the following spectral features in this section. At low frequencies (below 1 eV) all the curves show a sharply rising low-frequency divergence. In the 1-5 eV region there is sharp structure in all alloys. At high frequencies ($h\omega > 4$ eV) the $\Delta\sigma$ spectrum has a sharp rise. The observed spectra were nearly linear over the 1 - 10 at.% concentration range.

We will discuss the interpretation of the $\Delta\sigma$ spectra in terms of three processes: (a) Modifications in the host density of states which can include a reduction due to the replacement of host atoms with the impurity atoms and shifts and broadening of host bands. (b) Absorption associated with the impurity density of states. This includes transitions from impurity states to host states and the modification of the intraband absorption due to the impurity. (c) Impurity-induced k-non-conserving interband absorption. In this process it is expected that optical edges can occur at frequencies corresponding to the separation of peaks in the host density of states and the Fermi level, and optical absorption peaks can occur at frequencies corresponding to the separation of occupied and unoccupied peaks in the host density of states.

Of these three processes, (a) and (b) have been considered by Beaglehole and Hendrickson[18] in analyzing and interpreting their reflectivity data from dilute AuFe alloys. From a theoretical standpoint, only process (b) has been usefully developed in the literature.[22] Several authors have considered the optical response within the Anderson model of dilute alloys.[19,20,21] They have only considered the case where the impurity is placed in a simple free electron-like band. Since the final states in our experiment consist of both s-p like states and d-like states these results cannot give a complete description of our data. For the transitions in which the final states are s-p like the result for $\Delta\sigma/c$ in terms of the impurity density of states, $\rho_s^I(E)$ is

$$\Delta\sigma = \sum_s \frac{c}{8\omega}\left[\frac{\omega_p^2 V^2}{\omega^2} + \omega_d^2\right] \int_{-\omega}^{o} dE \;\; \rho_s^I(E) \qquad (3)$$

where c is the impurity concentration and s is the electron spin. ω_p is the effective plasma frequency associated with the s-p band and is 8.4 eV for Mo. ω_d is related to the d-s matrix element for the impurity and it can be estimated from the strength of the interband edge in pure Au to be of order 2-3 eV.

The low-frequency divergence in $\Delta\sigma$ can be interpreted largely in terms of the increased scattering of the conduction electrons in the alloy. The contribution of the Drude term to the conductivity is

$$\sigma = \frac{\sigma_o}{1 - i\omega\tau} \qquad (4)$$

where $\sigma_o = ne^2\tau/m^*$. At the frequencies we are dealing with $\omega\tau >> 1$ and so we can approximate (for the sake of discussion)

$$\text{Re}\ \sigma \simeq \frac{\sigma_o}{(\omega\tau)^2} \frac{1}{4\pi} \frac{\omega_p^2}{\omega^2} \frac{1}{\tau} \quad . \tag{5}$$

Therefore $\Delta\sigma \simeq \frac{1}{4\pi} \frac{\omega_p^2}{\omega^2} \Delta(\frac{1}{\tau})$. Eq. 5 clearly gives us a low-frequency divergence in $\Delta\sigma$ as observed experimentally. However, we should subtract from this a term $c(\sigma_P - \sigma_D)$ where σ_P stands for σ_{pure}, and σ_D is the Drude part of the conductivity of the pure sample. When this subtraction is performed from $\Delta\sigma$ calculated from Eq. 5 using $\Delta(1/\tau)$ estimated from the dc resistivity, we get reasonable agreement with the observed low frequency behavior of Δc for the alloys. From Figures 3, 4 and 5 we see that $1/\tau$ for the alloys gets progressively larger as the valence difference between the host and impurity increases. This behavior is in direct contradiction to the virtual bound state model for alloys as can be seen from Eq. 3. Since the peak in $\rho_s^I(E)$ should move farther away from the Fermi level for impurities Re, Os and Pt $\rho_s^I(0)$ should decrease respectively. Therefore the first term in Eq. 3 would decrease across the series in contrast to the observation. The observed behavior is more consistent with the idea that the electron relaxation rate will increase as the valence electron number difference (i.e. d-electron difference) increases because the impurity than provides a larger perturbing potential.

During the last six months of this research program one of the principle investigators (H. D. Drew) visited the University of California at Irvine in order to collaborate with Prof. D. Mills on some theoretical questions concerned with the interpretation of the optical experiments. The result of this was an examination of the role of k-nonconserving processes in the alloy induced by the addition of the impurities.[22] Qualitatively, these processes should lead to the following bands of structures: (1) peaks in $\Delta\sigma$ corresponding

to a transition from a peak in the density of states of the host below E_F to a peak above E_F, (2) edges in $\Delta\sigma$ corresponding to transitions from peaks in the density of states of the host below E_F to the Fermi level or transitions from the Fermi level to peaks in the density of states above E_F. These structures were looked for with the guidance of band calculations which indicate where the peaks in the Mo density of states should lie. The structures in the $\Delta\sigma$ data do not correlate well with the expectations of this model. However, the theory of the k-nonconserving process is more complex than indicated above and a more definitive evaluation must await realistic calculations based on the Mo bond structure.

The structures in $\Delta\sigma$ do correlate well with the expectations of process (a) above. Since Mo atoms are being replaced by the solute atom a proportionate decrease in σ is expected as one component of the change in σ. In the simplest model this contribution would go like $\Delta\sigma \approx -c\sigma_{pure}$. Therefore the peaks in the Mo spectrum at 1.7, 2.3 and 3.8 eV should give rise to corresponding dips in $\Delta\sigma$. The dips in the observed spectra are in approximately the correct positions and, the first two at least, are of approximately the correct magnitude. The 3.8 eV peak is anomalous in that it shifts steadily to higher energy and grows larger with increased valence difference.

Now we must discuss the contribution due to the valence electrons of the impurity atoms. It is generally expected that the impurity d levels in these types of alloys are not sharp virtual levels since they fall within the high density of d states of the host. Coherent-potential-approximation (CPA) calculations on NiCu alloys and AgPd alloys indicate broad densities of states function for the Cu and Ag in the Ni and Pd rich phases. Therefore we do not expect sharp features in the $\Delta\sigma$ spectra from the impurity electrons.

Also, from the behavior of $1/\tau$ discussed earlier it appears that there is significant potential scattering in these alloys which increases with valence difference. This potential scattering will account for some of the impurity electrons because a s-p scattering phase shift implies an s-p like density of states around the impurity atom by the Freidel sum rule.

The MoOs spectrum suggests a broad d-like contribution to $\Delta\sigma$ located around 2-3 eV. This and the $-c\sigma_{pure}$ contribution would account for the small net $\Delta\sigma$ in the 1.5-4 eV range. However, this model does not generalize for the other alloys. Indeed the large negative peak for MoPt near 4 eV suggests another type of interpretation. The 3.8 eV peak in pure Mo results from transitions between nearly parallel d-like bands over a large region of k-space. The large dip could arise from a shift of the lower band toward the Fermi level causing the oscillator strength near 4 eV to effectively shift to 2 eV. Such a shift would be consistant with a large s-p density at the Pt site in this alloy.

The MoRe alloy results are more difficult to interpret. The negative $\Delta\sigma$ between 1 and 5 eV is too large to be due to just the $-c\sigma_{pure}$ component. On the other hand the shape of $\Delta\sigma$ is remarkably close to this explanation. There does not seem to be any d-like contribution at all below 5 eV and it is hard to understand why that contribution would occur at high photon energies.

In conclusion, we have made a series of careful measurements of this differential reflectance between alloys of MoRe, MoOs and MoPt referenced to pure Mo in the optical spectral range. The differences in the resulting $\Delta\sigma$ spectra are distinctive but as yet yield no definitive conclusions on the electronic structure of these alloys. It is suggested that the s-p

density at the impurity site increases with increasing valence difference from the host. However, further interpretation must await more theoretical input. Indeed, these data should provide vital clues to the theorists. A preliminary report on the Mo-Re data has been published.[23] The work on the Os and Pt alloys was reported an APS meeting.[24]

III. Computer Studies of Peierls Stress

In the initial research proposal it was proposed that an investigation of the Peierls stress be undertaken based on an atomistic computer calculation. These atomistic calculations were to be based on interatomic potentials, and in the case of alloys a different interatomic potential was to be assigned to the solute atom. Due to the limitation of the support (time and money) it was concluded that the only way any progress could be made in these calculations was to obtain someone's existing program for making such calculations and modifying it to take into account the presence of solute atoms. A program was obtained from Dr. P. Gehlen. After much effort we were able to run it on our computer, however, in order to do so we had to insert a boundary condition. Later it was determined that this boundary condition prevented a determination of Peierls stress.

Concurrent with efforts to obtain the Peierls stress from the interatomic potential, a computer simulation investigation was undertaken of the interaction of an edge and screw dislocation and a size and modulus misfit, where the Peierls stress is zero (i.e., represent f.c.c. alloys) and also a computer simulation investigation of interaction of size modulus misfit interactions with a screw dislocation in a lattice containing a large Peierls stress (representing b.c.c. alloys).

Based on the interaction of the screw dislocations with randomly distributed solute atoms, the present results demonstrate that the double-kink mechanism would predict both solid solution weakening and strengthening. In Figure 7, the yield stress at 0° K required to overcome the

opposing force due to solute-dislocation interaction is shown to be lower than that of the double-kink nucleation in the absence of the solute atoms. As the concentration of the solute atoms increases, the yield stress for the double-kink nucleation decreases. In other words, if the rate controlling mechanism of dislocation motion is the nucleation of double kink, then solution weakening takes place as a result of solute additions. Figure 7 also shows that the stress required for the sideward motion of a kink is zero in the absence of solute atoms. As the concentration of solute atoms increases, the stress required for the sideward motion of a kink also increases. In other words, if the rate controlling mechanism of dislocation motion is the sideward motion of a kink, the solution strengthening takes place by the additions of solute atoms. For a given solute concentration, the yield stress first decreases to a minimum and then begins to increase for large values of ε_t where ε_t represents the size and modules misfit. For a given ε_t, that is, a given alloy system, the yield stress first decreases to a minimum then starts to increase with increasing solute concentration. Qualitatively, it is in agreement with the general trend of the experimental observations.

It is believed that the strength of the solute-dislocation interaction is determined by the modulus which describes the stress field of the dislocation. The modulus for screw and edge dislocations in b.c.c. metals, k33, has been expressed in terms of the elastic constants by Head. Therefore, k33 instead of G(1) and G(2) for the solute and solvent atoms was used to calculate the interaction parameters for modulus interaction. The elastic constants of the Ta-based alloys have been measured using the resonance technique by Armstrong and Mordike. This makes the

quantitative comparison for Ta-based alloys possible. The misfit-strains, ε, of the alloys are calculated from Mordike. The interaction parameters, M, for modulus interactions are calculated from the measured value of $d'(G,c)/G(1)$ as follows:

For elastic spheres of modulus G(2) imbedded in a matrix of modulus G(1), the measured value of $d'(G,c)$ should be:

$$\frac{dG}{dc} = \frac{2[G(2)-G(1)]G(1)}{(1+u)G(1)+(1-u)G(2)}$$

$$u = \frac{\nu(1) - \frac{1}{5}}{3(1-\nu(1))} \qquad (1)$$

From equation 1, the interaction parameter M can be written as follows:

$$M = \frac{\varepsilon(M)}{15(1-\nu(1))}$$

$$\varepsilon(M) = \frac{1}{G(1)} \frac{dG}{dc} \qquad (2)$$

where $\nu(1)$ is the Poisson's ratio of the solvent crystal. By substituting the corresponding k33 for G(1) and G(2) in the above equations, a comparison with experimental results can be made. The experimental data of Ta-based alloys by Braithwaite, Mordike and Rogausc.. ·r 3.5% solute concentration at 77 K is also plotted in Figure 8, where $\tau(p)$ was given the value of the yield stress for the pure Ta at 77 K. Quantitatively, it is in fair agreement with the numerical results.

Other experimental results for comparisons are the Mo-based alloys. An investigation was conducted by Stephens and Witzke to determine the effects of alloy additions on the hardness of Mo-based alloys. Because there are no adequate data of the shear moduli for the solute atoms, in the case of Mo alloys, the shear modulus of the solute and the solvent

crystals were derived from the Young's modulus of the polycrystals by using the relationship $G(i) = (\text{Young's modulus})/2/(1+\nu(i))$. The experimental results of micro-hardness tests for Mo-based alloys and the numerical results are shown in Figure 8. Qualitatively, it is in agreement with the general trend of the numerical results. Recently the hardness behaviour of nineteen binary iron alloy systems was investigated by Stephens and Witzke. Their results indicate that:

(1) The size effect plays a dominant role in controlling the hardness behaviour of binary iron alloys.

(2) Alloy softening does not occur in binary Fe-Zr and Fe-Hf systems because of the very large size difference between solute and solvent atoms, that is, the large interaction parameter. This is another evidence supporting the general trend of the present numerical results.

References

[1] J. R. Stephens and W. R. Witzke, J. Less-common Metals 29 371 (1972).

[2] J. Friedel, in Proceedings of the International School of Physics "Enrico Fermi" Course 37, Theory of Magnetism in Transition Metals, edited by W. Marshall (Academic, New York, 1967).

[3] H. Ehrenreich and L. M. Schwartz, in Solid State Physics, edited by H. Ehrenreich, F. Seitz, and D. Turnbull (Academic, N. Y., 1976). Vol. 31.

[4] H. D. Drew and R. E. Doezema, Phys. Rev. Lett. 28, 1581 (1972).

[5] B. Y. Lao, R. E. Doezema, and H. D. Drew, Solid State Commun. 15, 1253 (1974).

[6] D. Beaglehole, Phys. Rev. B 14, 341 (1976).

[7] M. Basset and D. Beagelhole, J. Phys. F 6, 1211 (1976).

[8] J. Lafait, thesis (unpublished).

[9] C. Norris and H. P. Myers, J. Phys. F 1, 62 (1971).

[10] B. F. Schmidt and D. W. Lynch, Phys. Rev. B 3, 4015 (1971).

[11] A. B. Callender and S. E. Schnatterly, Phys. Rev. B 7, 4385 (1973).

[12] J. P. Ferraton, G. Leveqne, and S. Robin-Kandare, J. Phys. F 5, 1433 (1975).

[13] S. Hüfner, G. K. Wertheim, and J. H. Wernick, Phys. Rev. B 8, 4511 (1973).

[14] D. Beaglehole, Appl. Opt. 7, 2218 (1968).

[15] B. W. Veal and A. P. Paulikas, Phys. Rev. B 10, 1280 (1974).

[16] D. D. Koelling, F. M. Mueller, and B. W. Veal, Phys. Rev. B 10, 1290 (1974).

[17] H. Ehrenreich and H. R. Philipp, Phys. Rev. 128, 1622 (1962).

[18] D. Beaglehole and T. J. Hendrickson, Phys. Rev. Lett. 22, 133 (1969).

[19] A. J. Bennett and D. Penn, Phys. Rev. B 11, 3644 (1975). These authors have considered the case with several bands, but not in a form that can be readily compared with experiment.

[20] B. Caroli, Phys. Kondens, Mater. 1, 346 (1963).

[21] B. Kjöllerström, Philos. Mag. 19, 1207 (1969).

[22] D. Mills-to be published

[23] S. K. Bahl and H. D. Drew, Phys. Stat. Sol. b 74, 721 (1976).

Figure Captions

Fig. 1 Evaporation geometry for sumultaneous preparation of pure and alloy film of predetermined composition.

Fig. 2 $\alpha = \frac{R_p - R_A}{R_p + R_A}$ for a Mo-Re alloy.

Fig. 3 $\omega\varepsilon_2$ vs $\hbar\omega$ for pure Mo.

Fig. 4 $\omega\Delta\varepsilon_2$ vs $\hbar\omega$ for a MoRe alloy.

Fig. 5 $\omega\Delta\varepsilon_2$ vs $\hbar\omega$ for a MoOs alloy.

Fig. 6 $\omega\Delta\varepsilon_2$ vs $\hbar\omega$ for a MoPt alloy.

Fig. 7 The yield stress at 0° K as a function of total interaction parameters. The yield stress was normalized to the Peierls stress of the base metal. The solid line represents the stress required for yielding if only double-kink nucleation is rate controlling, and the dashed line represents the stress required for yield if only lateral motion is rate controlling.

Fig. 8 Comparison of experimental results of micro-hardness tests for Mo-base alloys with the numerical results.

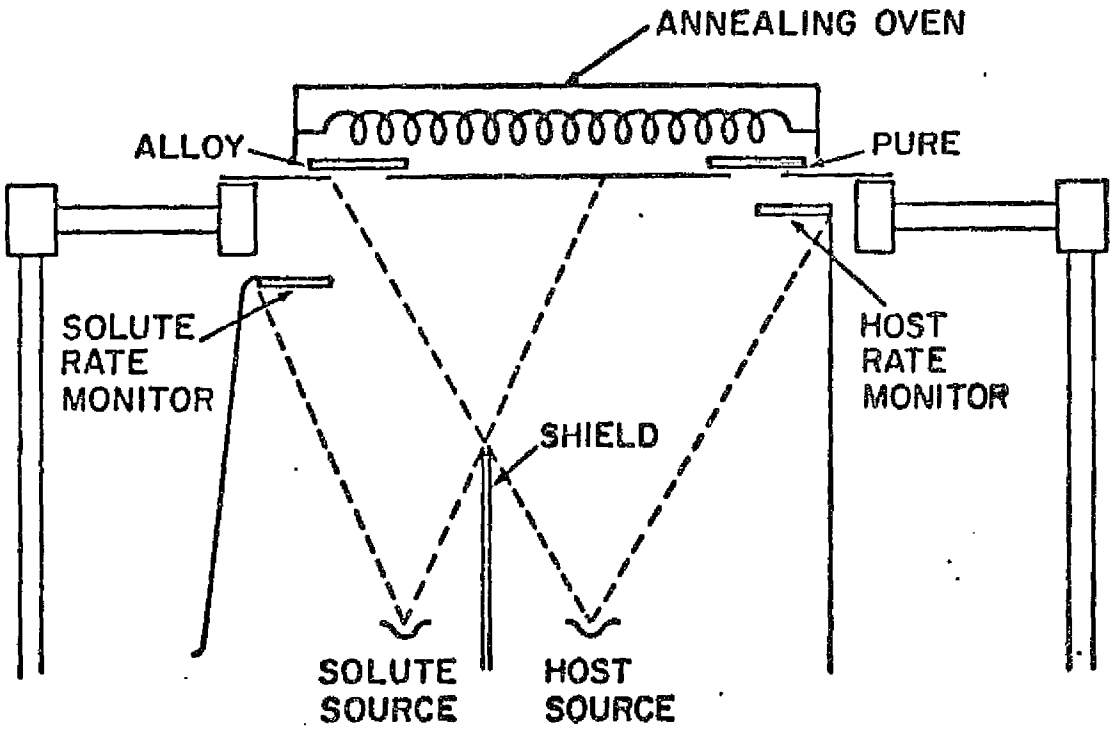

Fig. 1

Evaporator geometry for simultaneous preparation of pure and alloy films of predetermined composition.

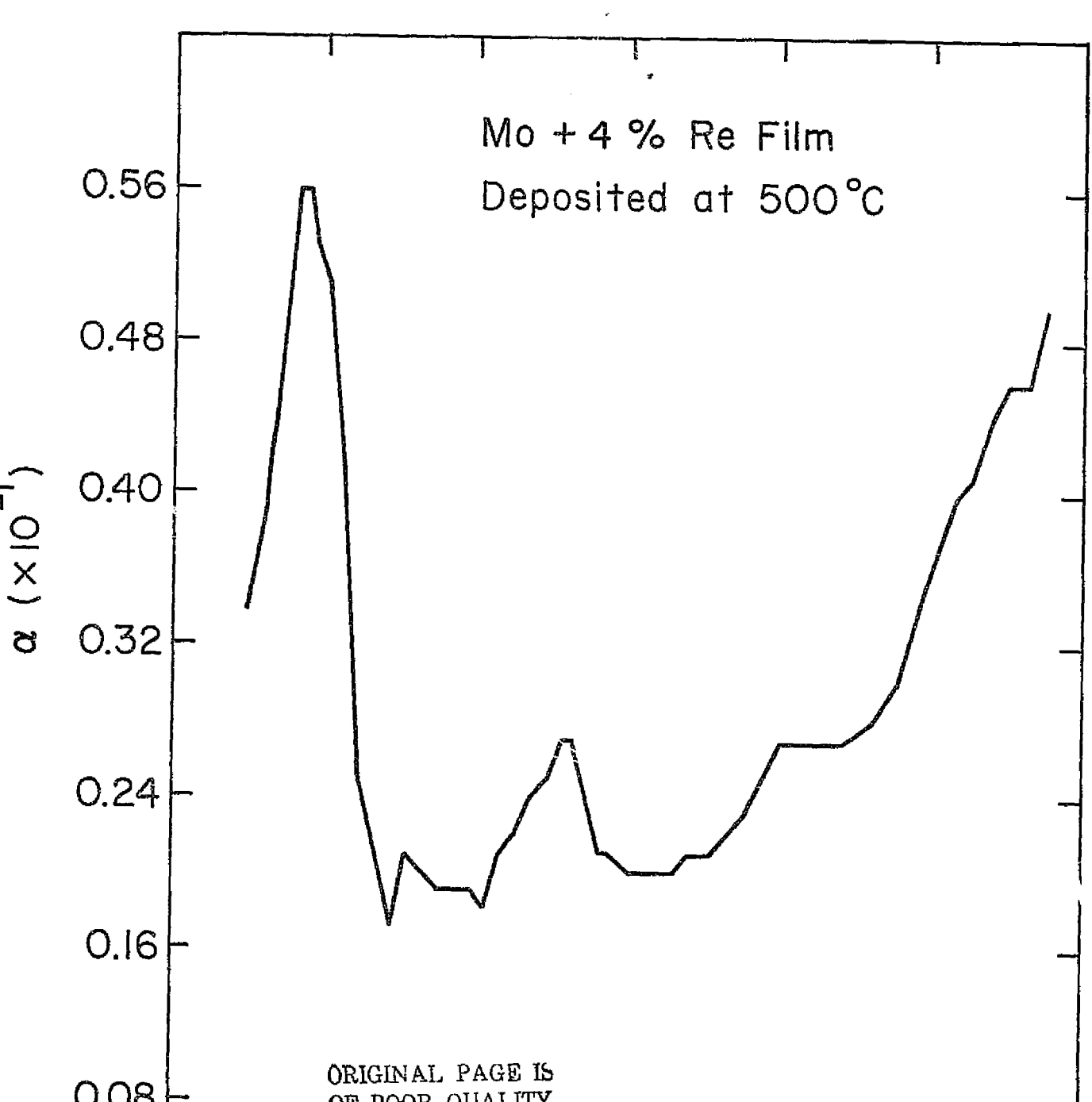
Mo + 4 % Re Film
Deposited at 500°C
0.56
0.48
0.40
0.32
0.24
0.16
0.08
0
α (×10⁻¹)
0
1
2
3
4
5
6
eV
ORIGINAL PAGE IS
OF POOR QUALITY

Fig. 2

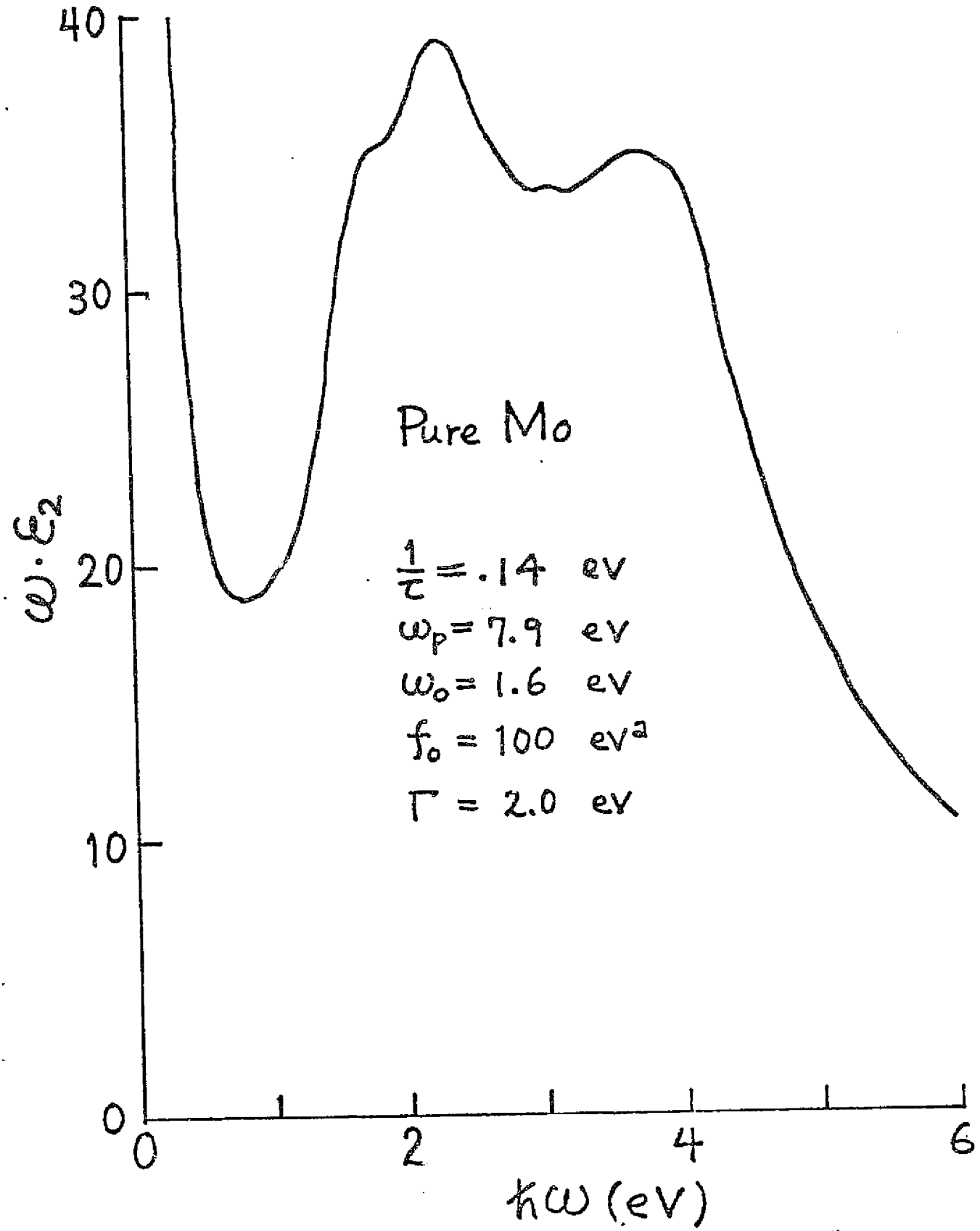

Fig. 3

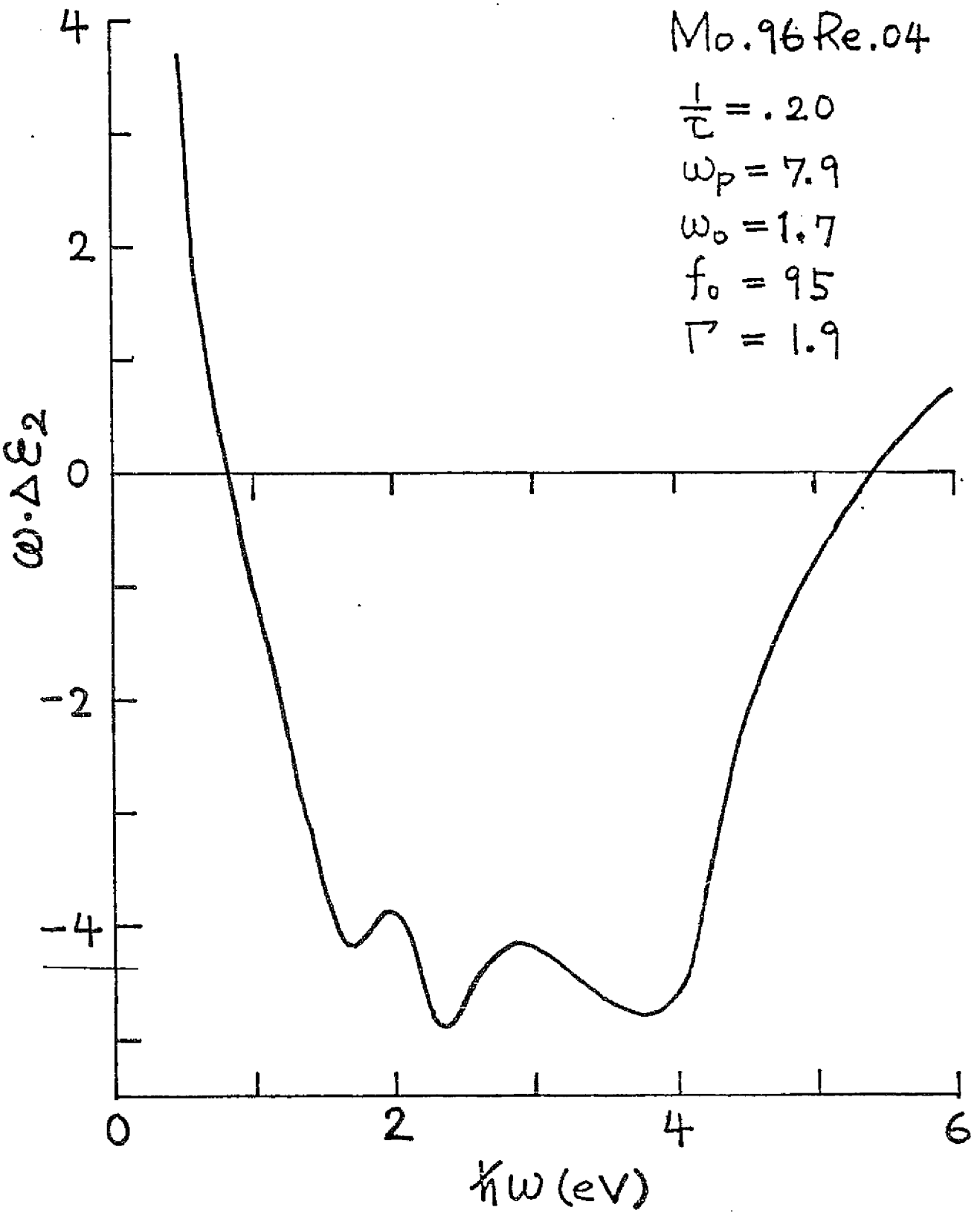
Mo.96Re.04
$\frac{1}{\tau} = .20$
$\omega_p = 7.9$
$\omega_0 = 1.7$
$f_0 = 95$
$\Gamma = 1.9$
$\omega \cdot \Delta\varepsilon_2$
4
2
0
-2
-4
0
2
4
6
$\hbar\omega$ (eV)

Fig. 4

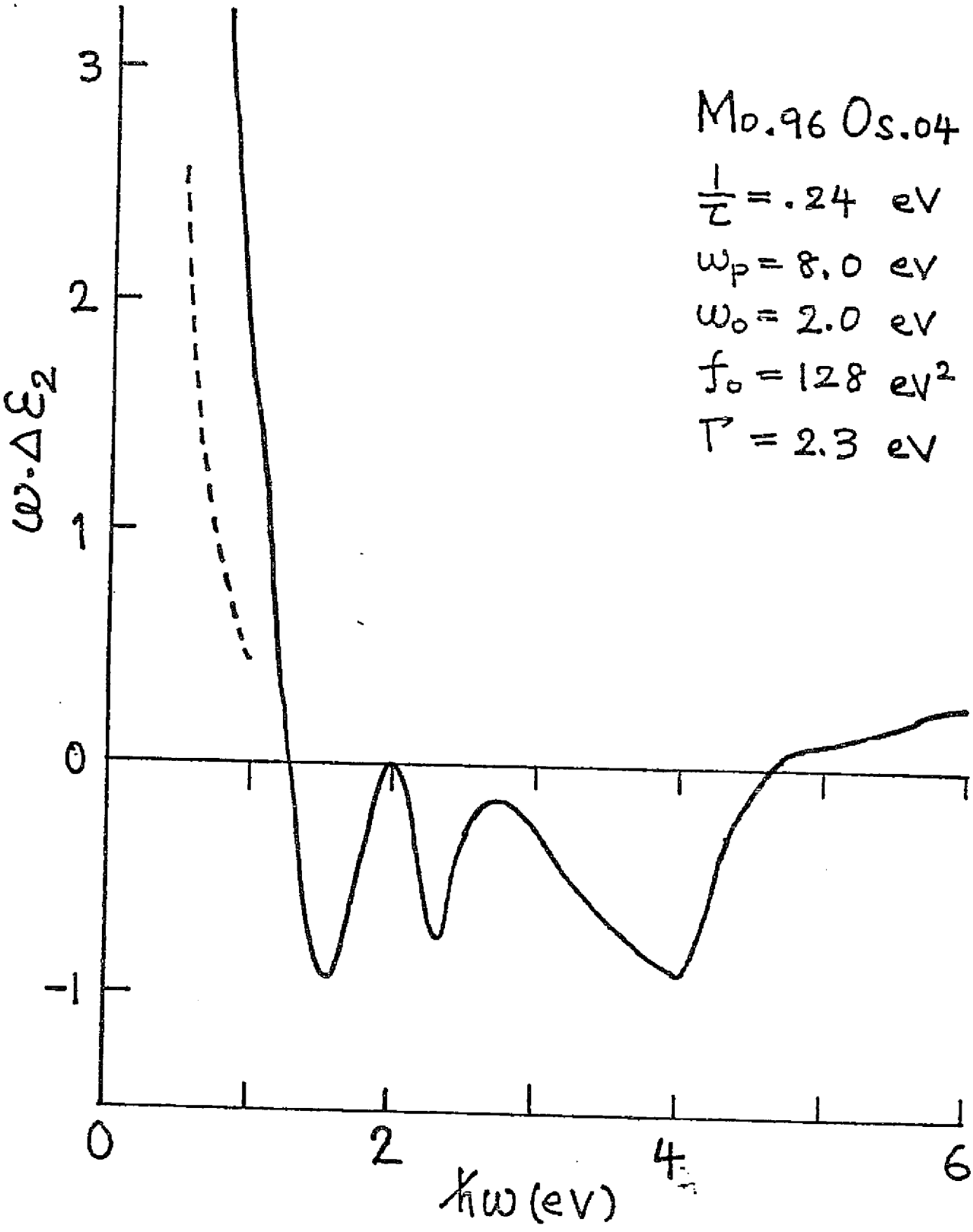
Mo.96 Os.04
1/τ = .24 eV
ω_p = 8.0 eV
ω_o = 2.0 eV
f_o = 128 eV²
Γ = 2.3 eV
ω·Δε₂
3
2
1
0
-1
0
2
4
6
ħω (eV)

Fig. 5

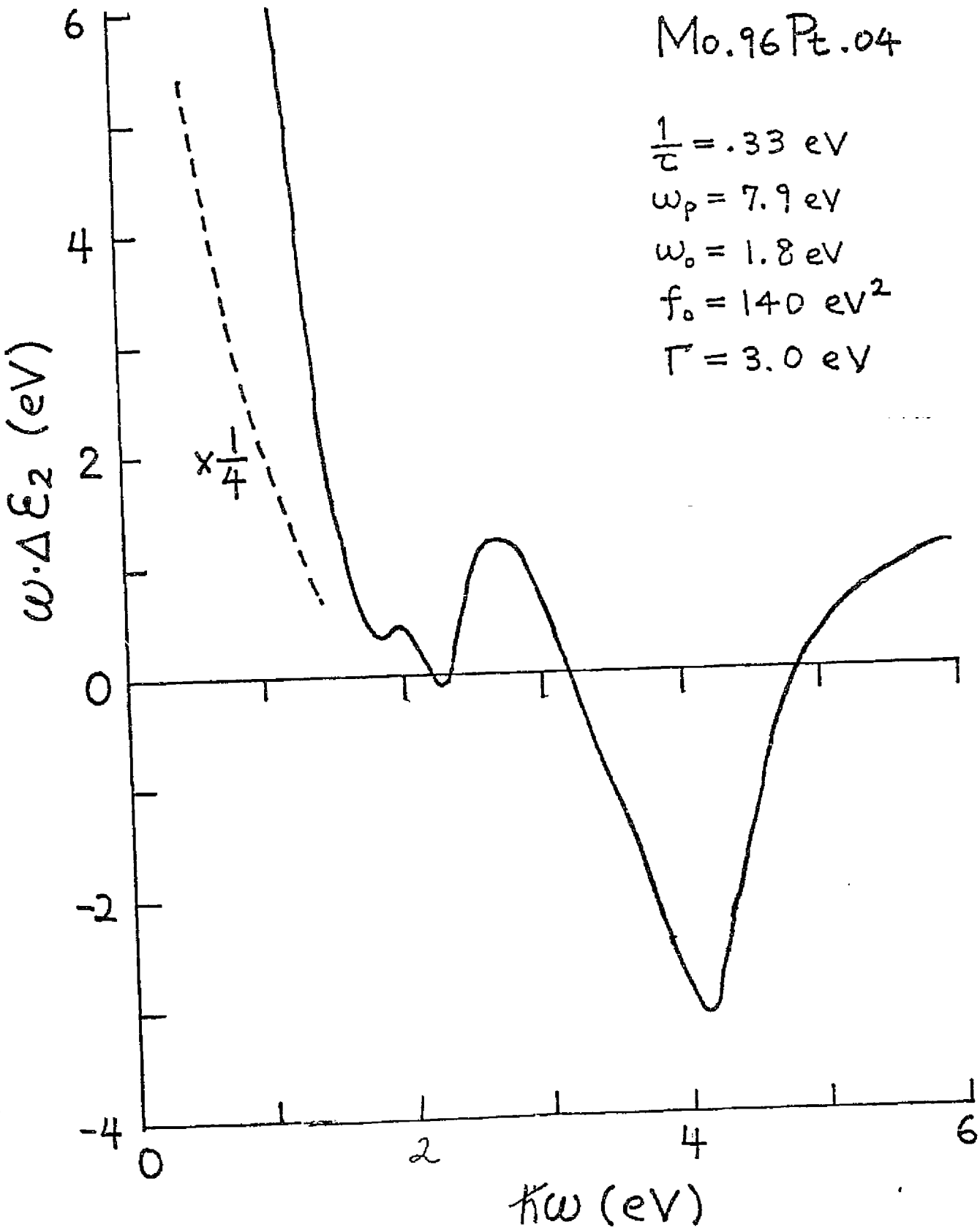
Mo.96Pt.04
$\frac{1}{\tau}$ = .33 eV
ω_p = 7.9 eV
ω_o = 1.8 eV
f_o = 140 eV^2
Γ = 3.0 eV
$\times\frac{1}{4}$
$\omega\cdot\Delta\varepsilon_2$ (eV)
$\hbar\omega$ (eV)
6
4
2
0
-2
-4
0
2
4
6

Fig. 6

phys. stat. sol. (b) 74, 721 (1976)

Subject classification: 20.1; 14.1; 21

Department of Physics and Astronomy, University of Maryland, College Park

Optical Properties of Mo–Re Alloys[1])

By

S. K. Bahl and H. D. Drew

Measurements of the reflectivity [R(pure) − R(alloy)] of 3000 Å thick Mo–Re films for photon energies between 0.54 and 6 eV and Re concentrations around 4 at% are reported. The resistivity of the films is also measured and 2.2 μΩ cm/at% is found for the change in resistivity of the films upon alloying. The frequency dependence of the optical dielectric function, $\varepsilon = \varepsilon_1 - i\varepsilon_2$, of the pure and alloy films is found from a Kramers-Kronig analysis of the reflectivity data. The results for the differential optical conductivity $\omega[\varepsilon_2(\text{alloy}) - \varepsilon_2(\text{pure})]$ are discussed in terms of the changes in the electronic structure of Mo upon alloying with Re. It is concluded that the rigid band model is inapplicable in this case. The results of the optical data and the resistivity are consistent with the formation of localized Re d-levels 0.8 eV below the Fermi level where pure Mo has a low density of electronic states. However, this interpretation is not unique and further studies are suggested.

Nous présentons des mesures de la reflectivité [R(pur) − R(aliage)] pour des couches de 3000 Å d'épaisseur, des energies du photon de 0.54 à 6 eV et une concentration de Re de 4%. Nous avons aussi mesuré une difference de resistivité entre l'élément pur et l'aliage de 2.2 μΩ cm/at%. La dépendance en fréquence de la function diélectrique optique $\varepsilon = \varepsilon_1 - i\varepsilon_2$ pour l'élément pur et l'aliage est determineé à partir d'une analyse de type Kramers-Kronig des résultats sur la réflectivité. La difference des conductivités optiques $\omega[\varepsilon_2(\text{aliage}) - \varepsilon_2(\text{pur})]$ est reliée aux changements de la structure électronique de Mo en aliage avec Re. On conclude que le model à bandes rigides ne s'applique pas dans ce cas. Les mesures peuvent s'expliquer par l'apparition locale de Re 0.8 eV en dessous du niveau de Fermi aux endroits où Mo pur a une faible densité d'états électroniques. Toutefois, cette interprétation n'est pas unique et une poursuite de ces traveaux semble approprieé.

1. Introduction

The question of the electronic structure of transition metal alloys is a difficult one that has nonetheless shown recent progress in both experimental measurements and theoretical studies [1]. The series of alloys consisting of Mo plus the 5d transitional elements is an interesting one that has received little attention to date. The solubilities are all sufficiently high to permit spectroscopic studies and therefore a systematic investigation of the electronic structure. Another interesting aspect of this alloy series is that their mechanical properties appear to be related to their electronic structure [2]. We have therefore undertaken a study of the optical properties of these alloys. As part of this objective we have carried out measurements of the optical properties of Mo–Re alloy films. The results of these studies are reported in this note.

2. Experimental Details

The Mo–Re alloy films were prepared by e-gun evaporation in a conventional oil diffusion pumped bell jar system having a liquid nitrogen cold trap. The base pressure of the system was typically $\approx 2 \times 10^{-7}$ Torr which rose to

[1]) Work supported by the National Aeronautics and Space Administration under Grant No. NSG 3001.

2×10^{-5} Torr during evaporation. The source for evaporation was a boule of $Mo_{0.92}Re_{0.08}$ provided by NASA Lewis Research Center. The films were deposited on optically polished fused quartz discs (1 in. diameter) preheated to 500 °C. The evaporation rate was ≈30 Å/s and the film thickness was typically 3000 Å. Pure molybdenum films were made by evaporation of high-purity Mo (MRC Marz grade) using deposition conditions similar to that used for alloy films. The composition of the alloy films was determined by wet chemical analysis and by X-ray fluorescence. The structure of the films was studied using X-ray diffraction, electron diffraction, and electron microscopy. The films were found to be polycrystalline with a lower limit on the crystallite size of 500 Å.

The optical measurements were made using a differential technique, i.e., by comparing the reflectivity of pure Mo film with that of the alloy film. The quantity $\Delta = (R_p - R_A)/(R_p + R_A)$ was measured in the energy range of 0.54 to 6 eV using an optical system similar to that described by Beaglehole [3]. R_p and R_A are the reflectivities of the pure and the alloy films, respectively. For the differential reflectivity measurements samples on 1 in. fused quartz discs were used. The spectral dependence of reflectivity of pure Mo films was measured using the reflecting stage of a Perkin-Elmer 350 spectrophotometer. Due to the geometry of the reflecting stage, it was not possible to make measurements on the 1 in. disc samples. Instead Mo films on 2×1 in.^{2} fused quartz slides were used. Reflectivities were found to be dependent on substrate deposition temperatures. Samples prepared at ≈ 500 °C substrate temperature were found to have reflectivities essentially identical to the best measurement [4] reported on bulk Mo.

Since the spectral dependences of Δ and R_p are experimentally measured, this allows us to obtain the reflectivity of the alloy as a function of photon energy. The resistance of the pure and alloy films was measured at room temperature and 4.2 K using the four probe method. From these results we deduced the change in resistivity upon alloying of $\Delta\varrho = 2.2\ \mu\Omega$ cm/at% for our films.

3. Results

The spectral dependence of Δ is shown in Fig. 1. Several films were studied whose nominal composition were the same. However, variation in the resulting amplitude of Δ indicates that the actual composition varied from film to film. For the film corresponding to Fig. 1 the composition was measured, by X-ray fluorescence, to be 4 at%. The spectral features in the optical data for different films were found to be identical. We estimate the range of compositions studied as 3 to 5 at%.

The optical constants were obtained from reflectivity data using a Kramers-Kronig analysis which requires appropriate low (<0.54 eV) and high (>6 eV) energy extrapolations of the reflectivity outside the experimental range.

The $\omega \to 0$ extrapolation was determined by assuming that the complex dielectric constant function (ε) could be expressed as a sum of Drude term and a single harmonic oscillator term whose centre ω_0 was above the low frequency cut off $\omega_1 = 0.54$ eV. Thus for the $\omega \to 0$ extrapolation, we have

$$\varepsilon(\omega) = 1 + \frac{\omega_p^2\tau}{-\omega^2\tau + i\omega} + \frac{f}{\omega_0^2 - \omega^2 + i\Gamma\omega}; \qquad \omega < \omega_1 . \tag{1}$$

The strength and width parameters f and Γ were taken as adjustable. The Drude

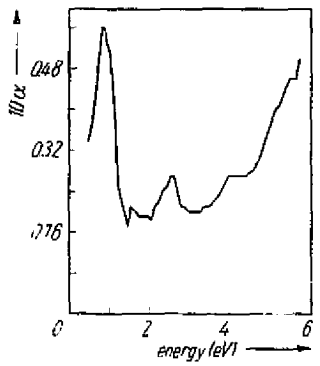

Fig. 1. Spectral dependence of $(R_p - R_A)/(R_p + R_A)$ of Mo + 4% Re alloy film deposite on 500 °C fused quartz substrate. The thickness of the film is approximately 3000 Å

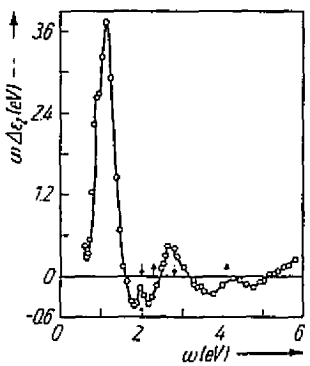

Fig. 2. Spectral dependence of $\omega\,\Delta\varepsilon_2$ of the film of Fig. 1 as obtained by Kramers-Kronig analysis. The arrows mark the peaks (↑) and dip (↓) in the conductivity for pure Mo

term in (1) can be calculated knowing the values of plasma frequency (ω_p) and relaxation time (τ) for the electrons. For Mo $\omega_p = 8.4$ eV, the value given by Veal and Paulikas [4] was used. τ was obtained by measuring the residual resistivity ratio (RRR) of ϱ at 4.2 to ϱ at 300 K. Assuming the conductivity is dominated by a free-electron-like portion of Fermi surface, we can write for the resistivity, ϱ

$$\varrho(300\ \mathrm{K}) = \frac{m}{ne^2}\left(\frac{1}{\tau_l} + \frac{1}{\tau_I}\right), \tag{2}$$

where τ_l and τ_I are contributions to relaxation time due to lattice vibrations and impurities and imperfections in the sample. Other symbols have their usual meaning. At low temperature the contribution to relaxation rate due to lattice vibration is expected to be insignificant. The RRR for the pure is therefore

$$\mathrm{RRR} = \frac{\tau_l}{\tau_l + \tau_I}.$$

τ_l is determined from the value of dc conductivity [5] of pure Mo which can be expressed as

$$\sigma_{\mathrm{dc}} = \frac{\omega_p^2 \tau_l}{4\pi}. \tag{3}$$

Using $\omega_p = 8.4$ eV, a value for $\tau_l/\hbar$ of 15.2 $(\mathrm{eV})^{-1}$ was obtained. Knowing τ_l, the value of τ_I and the relaxation time for the film can be determined from the RRR of the sample. For the pure film corresponding to the data of Fig. 1 and 2 we found $\tau_{\mathrm{pure}} = 9.1\ (\mathrm{eV})^{-1}$.

It is assumed for the alloy film that the solute adds another scattering mechanism, and then the relaxation rate of the alloy can be found by a similar analysis of its RRR. τ_{alloy} was found to be 4.4 $(\mathrm{eV})^{-1}$.

From values of ω_p and τ, the spectral dependence of Drude term in (1) was calculated. Then the parameters f and Γ were chosen, taking $\omega_0 = 1$ eV, to match R and $\mathrm{d}R/\mathrm{d}\omega$ at $\omega_1 = 0.54$ eV for the pure Mo and the alloy films. This analysis was performed to provide a consistent low-frequency extrapola-

tion. The results for $\Delta\varepsilon_2 \equiv \varepsilon_2$ (alloy) $- \varepsilon_2$ (pure) were not very sensitive to the assumptions made in this analysis.

The values obtained for parameters f and Γ were, respectively, 198.5 $(\mathrm{eV}/\hbar)^2$ and 1.64 $\mathrm{eV}/\hbar$ for Mo, 184 $(\mathrm{eV}/\hbar)^2$ and 0.67 $\mathrm{eV}/\hbar$ for the alloy films.

For the $\omega \to \infty$ extrapolation it is assumed that the reflectivity varies as

$$R = R_h \left(\frac{\omega_h}{\omega}\right)^q \tag{4}$$

for $\omega \geqq \omega_h$. R_h is the measured reflectivity at the highest measured energy $\omega_h = 6$ eV. The parameter q was varied until the sum rule $\left(\int_0^\infty \omega\, \Delta\varepsilon_2\, d\omega = \right.$ $\left. = 2\pi^2 N e^2/m\right)$, where N is total number of valence electrons/cm^3) was satisfied. For a pure Drude metal above the plasma frequency or for the energy region well above the interband transition energy, q is expected to be 4. In our case the sum rule required $q = 2.552$ for Mo and $q = 2.522$ for the alloy. This indicated that we had not exhausted all the interband transitions at 6 eV. The small difference in value of q of the alloy is due to extra concentration of electrons due to the addition of Re.

The energy dependence of $\omega\, \Delta\varepsilon_2$ obtained by the Kramer-Kronig analysis is shown in Fig. 2. The most prominent feature in the spectrum is the sharp peak at about 1.1 eV. However, the smaller structures for energies >1.5 eV are significant features as they reproduce for different alloy films.

4. Discussion

According to Koelling et al. [6] the absorption edge observed [4] in Mo at ≈ 1.5 eV involves states at E_F. They concluded that if this edge is considered in terms of direct transitions (requiring k-conservation) this would involve states from E_F to states at higher energy. If, on the other hand, indirect transitions prevail, transitions from peak in the density of states at ≈ 1.5 eV below E_F to states near E_F are to be considered. In terms of the rigid band model alloying Mo with Re (containing one extra d-electron) should produce the equivalent of an upward shift of E_F. In the direct transition model, an upward shift of E_F should produce a positive peak in $\omega\, \Delta\varepsilon_2$ at 1.5 eV, and for indirect transitions, this shift would lead to a negative peak in $\omega\, \Delta\varepsilon_2$ at 1.5 eV. Since no structure in $\omega\, \Delta\varepsilon_2$ is observed at 1.5 eV, the reflectivity data is therefore inconsistent with the rigid band model.

Another plausible idea for understanding of the alloy data is in terms of the broadening of the 1.5 eV Mo edge [6] upon alloying. Broadening of the edge will give a positive peak below 1.5 eV and a negative peak above 1.5 eV in $\omega\, \Delta\varepsilon_2$. This idea seems to be qualitatively consistent with the data. In fact a symmetric positive and negative peak of roughly equal magnitude should be expected around 1.5 eV. The smaller values of the negative peak above 1.5 eV could be due to the interference of this structure with other interband structure at higher energies. From the change in the slope of the absorption edge of the alloy as compared to Mo it is estimated that the edge is broadened ≈ 0.1 eV. The change in $\hbar/\tau$ (as obtained from resistivity ratio) is 0.1 eV, a value similar to that obtained for the broadening parameter. This suggests that the broadening may arise from electron lifetime effects upon alloying.

On the other hand it appears that the peak in $\omega\, \Delta\varepsilon_2$ is rather too low (i.e. ≈ 1.1 eV) to be considered part of the edge which has a foot at ≈ 1.24 eV [4, 6].

Another possible interpretation of the data is in terms of transitions from localized impurity levels on the Re sites. Thus if the Re d-levels were located about 0.8 eV below E_F the leading edge of the peak in $\omega \Delta\varepsilon_2$ could come from the onset of transition from this level to states above E_F. For a narrow impurity level at E_0 we expect [7, 8]

$$\omega \Delta\varepsilon_2 = \theta(\omega - E_0) \frac{5\pi\omega_d^2}{\omega} \frac{N_0}{10}, \tag{5}$$

where θ is the step function, N_0 is the number of impurity states at E_0 and ω_d is related to the optical matrix element for the transitions from these states. In addition we would expect a reduced contribution from the Mo interband transition because of the reduced Mo concentration in the alloy. The simplest assumption for this contribution is a term $\omega \Delta\varepsilon_2 \approx -c\omega\varepsilon_2$(pure), i.e., a uniform reduction in $\omega \Delta\varepsilon_2$ where c in the solute concentration is in at%. Evidence for this type of contribution is found in Fig. 2. There are peaks in $\omega\varepsilon_2$ (pure) at 2.3 and 4.1 eV and dips at 2.0 and 2.8 eV as indicated on the figure. A good anticorrelation of these features with the fine structure in $\omega \Delta\varepsilon_2$ is seen. In this model, we understand the rapid drop in $\omega \Delta\varepsilon_2$ near 1.5 eV as a consequence of the optical edge in Mo.

For $N_0 = 10$, $\omega_d = 3$ eV, equation (5) predicts $\omega \Delta\varepsilon_2 = 7$ eV at $\omega = 1$ eV. The experimental value of $\omega \Delta\varepsilon_2$ is 3.6 eV. $\omega_d = 3$ eV is close to the value deduced [9] from the interband edge in Au and Cu d → s transitions. On the other hand N_0 should be less than 10. As there are only 6d electrons in Re having ten filled states at an impurity level 0.8 eV below E_F would lead to an excess negative charge on the impurity. However, from the point of view of generalized Anderson model [10] the impurity density of states is given by

$$D(\omega) = \frac{\pi^{-1} \Delta(\omega)}{(\omega - E_0 - \Lambda(\omega))^2 + \Delta^2(\omega)}, \tag{6}$$

where the width function $\Delta(\omega) = \pi |V_{kd}|^2 D_p(\omega)$ and $D_p(\omega)$ is the host electronic density of states and $\overline{|V_{kd}|^2}$ is an average of the mixing matrix element. $\Lambda(\omega)$ is the level shift function [10]. If $\omega - E_0 - \Lambda(\omega)$ has a root near 0.8 eV below E_F, where $D_p(\omega)$ has a minimum, Δ should therefore be small. From (6) we see that $D(\omega)$ would therefore be very large near this energy. Moreover, as $D(\omega)$ would be expected to have weight throughout the s-d band width in Mo we might expect some weight above E_F which would enable the satisfying of the charge neutrality of the impurity.

The value of $\Delta\varrho/c$ ($\Delta\varrho = \varrho_{alloy} - \varrho_{pure}$) also gives some information about the electronic structure of the alloy which we can illustrate by the following oversimplified analysis. If we assume that the conductivity is dominated by a free-electron-like band characterized by the plasma frequency measured by Veal and Paulikas we can write [11]

$$\frac{\Delta\varrho}{c} = \frac{4\pi}{ze^2 k_F} \sum_l (l+1) \sin^2(\delta_l - \delta_{l+1}),$$

where z is the number of conduction electrons per atom (for $\omega_p \approx 8.4$ eV, $z \approx 1$), k_F is the effective Fermi momentum of the conduction electrons and the δ_l are the phase shifts evaluated at the Fermi level. Assuming that the resistivity dominated by δ_2 because of the d-character of the impurity atom and taking

$k_F \approx 1.3 \times 10^8$ cm as representative (this is typical of the noble metals) we get

$$\frac{\Delta\varrho}{c} = 20 \sin^2 \delta_2 \, \mu\Omega\,\mathrm{cm/at\%}.$$

This has a maximum value of 20 $\mu\Omega$ cm when δ_2 is $\pm\pi/2$ corresponding in the Anderson-Friedel model to a virtual bound state located at the Fermi level. Since the measured $\Delta\varrho/c$ of 2.2 $\mu\Omega$ cm/at% is nearly an order of magnitude smaller we take this to indicate that the density of d-states of Re at E_F is not high. This argument is only suggestive because of the assumptions made in the analysis. However it is consistent with the interpretation of the optical data in terms of a localized level 0.8 eV below E_F.

5. Concluding Remarks

We see that the differential optical properties of Mo-Re alloys has two kinds of interesting features. Structure above 1.5 eV that seems to indicate an overall reduction in the Mo density of states and a large peak near 1 eV that has two possible interpretations. First, it could arise from localized Re d-states located in the valley of the host density of states between the bonding and anti-bonding orbital peaks in the density of state. The second possibility is that this peak comes from a broadening of the 1.5 eV optical edge in Mo upon alloying. For this interpretation we are left with the question of where the impurity states are located. In particular, the electrical resistivity of the alloys indicates that the density of impurity d-levels at the Fermi level is small. Experiments on other alloys of Mo with 5d transition elements would be helpful in distinguishing between these different interpretations. We have attempted to study MoOs, MoPt, and MoHf alloys by the same technique but without success because the difference in the evaporation rates for the constituents of the alloy were too great to produce useful films. We are modifying our evaporator to permit simultaneous evaporation of the constituents to enable further study of this alloy series.

Acknowledgements

We wish to thank the Center for Materials Science of the University of Maryland for use of their X-ray diffraction and electron microscope facilities. We also thank J. Stephens of NASA Lewis Research Center for supplying the bulk alloys.

References

[1] A. Bansil, H. Ehrenreich, L. Schwartz, and R. E. Watson, Phys. Rev. B 9, 445 (1974).
[2] J. R. Stephens and W. R. Witzke, J. less-common Metals 29, 371 (1972).
[3] D. Beaglehole, Appl. Optics 7, 2218 (1968).
[4] B. W. Veal and A. P. Paulikas, Phys. Rev. B 10, 1280 (1974).
[5] Handbook of Chemistry and Physics, 53rd ed., Chemical Rubber Comp. Press, Cleveland (Ohio) 1972 (p. F145).
[6] D. D. Koelling, F. M. Mueller, and B. W. Veal, Phys. Rev. B 10, 1290 (1974).
[7] B. Caroli, Phys. kondens. Materie 1, 346 (1964).
[8] B. Kjollerstrom, Phil. Mag. 19, 1207 (1969).
[9] D. Beaglehole and E. Erlbach, Solid State Commun. 8, 255 (1970).
[10] D. M. Newns, Phys. Rev. 178, 1213 (1969).
[11] See, for example, E. Daniel and J. Friedel, in: Proc. IX. Internat. Conf. Low-Temperature Physics, Ed. J. Daunt, P. Edwards, F. Malford, and M. Yaqub, Plenum Press, New York 1965 (p. 933).

(Received January 5, 1976)

BP 77-209

J. Phys. C: Solid State Phys., Vol. 10, 1977. Printed in Great Britain. © 1977

Analysis of Kramers–Kronig relations in modulation spectroscopy

R E Prange,† H D Drew‡ and J B Restorff§

Department of Physics and Astronomy, University of Maryland, College Park, Maryland, USA

Received 28 March 1977

Abstract. A new method of extrapolation in the analysis of Kramers–Kronig relations, applying to the case of modulation spectroscopy, is presented. The extrapolation of the differential reflectance, $\Delta R/R$, is avoided, since this quantity is not theoretically the simplest, and it depends on unmodulated optical constants in an essential way. Rather, the extrapolation is made directly in the quantity of greatest theoretical simplicity, the real part of the (differential) optical conductivity itself. A formula is found which gives the differential optical conductivity in terms of the measured differential reflectivity and the extrapolated conductivity. The results are discussed and illustrated by the example of the optical conductivity of tungsten, modulated by a chemisorbed hydrogen layer.

The Kramers–Kronig dispersion relations (KKR) connecting real and imaginary parts of the Fourier transform of response functions (susceptibilities) are important in all branches of physical science. The KKR express the analytic properties in frequency space equivalent to the causal properties of the time-dependent response functions.

One of the uses of the dispersion relations arises because the susceptibility of greatest interest may not be directly measured. Rather, the real part of some analytic function of the basic susceptibility is measured. In order to invert the functional relation the full complex function is needed, i.e., the imaginary part is needed in addition to the measured real part. The KKR is used to compute the imaginary part.

As an example, the fundamental response function (in the long-wavelength or local limit) of a solid, may be taken to be the complex conductivity $\sigma(\omega) = \sigma'(\omega) + i\sigma''(\omega)$. The KKR is

$$\sigma''(\omega) = -\frac{2\omega}{\pi} \mathrm{P} \int_0^\infty \sigma'(t)\, \mathrm{d}t/(t^2 - \omega^2).$$

Greatest interest attaches to $\sigma'(\omega)$, as this quantity is the easiest one to estimate and interpret. However, σ' is not measured directly. Rather, the simplest experiments are capable of measuring only the reflectivity R, given by $R = |r|^2 = |(n-1)/(n+1)|^2$ with $n = [1 + 4\pi\, i\sigma(\omega)/\omega]^{1/2}$. It is well known that, with $r = R^{1/2}\, e^{i\theta}$, a KKR connecting the

† Work supported in part by NSF Grant DMR-75-13911A01.
‡ Supported in part by ARPA Grant No DAHC 04-75-G-0141.
§ Permanent Address: Naval Surface Weapons Center, White Oak, Maryland, USA.

real and imaginary parts of $\ln r$ exists, i.e. a relation determining $\theta(\omega)$ from an integral over $\ln R$.

In practice a difficulty immediately arises, since R is measured over a finite frequency range. It is necessary then to extrapolate $\ln R$ outside the measured range, on the basis of theoretical and phenomenological considerations. If the measurements have reached asymptotia, or alternatively if one is interested only in sharp structure in σ' which is little influenced by the extrapolation, this program can be highly successful. On the other hand, there are many cases of interest in which there is a significant contribution to σ' in the unmeasured region, and where σ'' has thus not reached its asymptotic form there.

On physical arguments, one may have a fair idea of how σ' behaves in the unmeasured region, but to extrapolate R on the basis of such a guess requires a tedious self-consistency procedure which is rarely attempted (D F Aspnes 1976, private communication). It would be useful therefore, to have a direct way of combining the measured values of R in one frequency range with extrapolated or guessed values of σ' in the remaining range, in order to give best values for σ' for all frequencies.

We have produced such a formula for the common case in which the measured quantity is a *linear* combination of the real and imaginary parts of σ. This case arises, for example, in modulation spectroscopy (Cardona 1969), where, in effect, the small difference between the reflectivities of two different samples is measured. Then, calling the difference of (effective) conductivities $\Delta\sigma$ we have

$$\Delta R/R = 2\,\mathrm{Re}\,(\Delta\sigma/n\sigma) \equiv \alpha\Delta\sigma' + \beta\Delta\sigma''. \tag{1}$$

The so-called Seraphin coefficients (Seraphin and Bottka 1966), α and β, may be calculated from a knowledge of the conductivity of the unmodulated sample, which is assumed to be known.

The problem which we have posed is: given (by measurement) α, β, and $\Delta R/R$ over a given frequency range L, (symmetrically extended to negative frequencies) and given (by extrapolation) $\Delta\sigma'$ over the remaining frequencies $R - L$, to find $\Delta\sigma'$ on L. This may be recognised as a problem of solving a singular integral equation. The solution is found by the methods expounded by Mushkelishvili (1953). The result is

$$\Delta\sigma' = 2\,\mathrm{Re}\lim_{\eta\to 0+}\Sigma(\omega + \mathrm{i}\eta) \equiv 2\,\mathrm{Re}\,\Sigma^{+}(\omega) \tag{2}$$

where

$$\Sigma(z) = \frac{X(z)}{2\pi\mathrm{i}}\left[\int_L \mathrm{d}t\,\frac{\Delta R/R\,(t)}{[\alpha(t) - \mathrm{i}\beta(t)]X^{+}(t)\,(t - z)} + \int_{R-L}\mathrm{d}t\,\frac{\Delta\sigma'(t)}{X^{+}(t)\,(t - z)} + P(z)\right]$$
$$(\mathrm{Im}\,z \neq 0). \tag{3}$$

Here

$$X(z) = (Q(z)/R(z))\exp\Gamma(z) \tag{4}$$

where

$$\Gamma(z) = \frac{1}{2\pi\mathrm{i}}\int_L \frac{\mathrm{d}t}{t - z}\ln\left(\frac{\alpha(t) + \mathrm{i}\beta(t)}{\alpha(t) - \mathrm{i}\beta(t)}\right) \tag{5}$$

and Q, R, as well as P are polynomials. The condition that $\Sigma(z)$ be finite everywhere in the complex plane, and the sum rule condition that it vanish as $\Delta\omega_p^2/4\pi z$ as $z \to \infty$, where $\Delta\omega_p^2$ is the modulation of the plasma frequency, determines P, Q, and R sufficiently to

give a unique solution. However, in general, for a solution to exist at all requires that certain additional sum-rule-like conditions be imposed.

The general case cannot be categorised succinctly, so we restrict consideration to the instance where $\phi(\omega) = -i \ln[(\alpha + i\beta)/(\alpha - i\beta)]$ may be taken as smooth (except possibly for a jump at the origin), odd in ω, and less in magnitude than 2π for $\omega \in L$. At least for the case of modulation spectroscopy it may be shown that ϕ has the above properties. In this case it is possible to choose $Q = R = 1, P = 0$ without loss of generality.

A number of points concerning the solution (3) may now be made.

(i) Since the relation is linear, knowledge of $\Delta R/R$ determines a certain 'experimental' contribution to $\Delta\sigma'$, which is non-zero only in the interval L. The effect of errors in $\Delta R/R$ may be readily discussed. The measured $\Delta R/R$ determines a unique contribution to the sum rule for $\Delta\sigma'$.

(ii) The contribution to $\Delta\sigma'(\omega)$ for $\omega \in L$ coming from the integral over $R - L$ may be calculated independently of the measured $\Delta R/R$, α, and β. Errors arising from poor choice of $\Delta\sigma'$ are easily discussed. The *total* contribution to the sum rule of the extrapolated $\Delta\sigma'$ is also determined independently. (It is not just $\int_{R-L} \Delta\sigma'\, d\omega$.)

(iii) The integrals encountered in equation (3), although improper, are well defined under physically realistic assumptions on $\Delta\sigma'$ and $\Delta R/R$. $X^+(\omega)$ for $\omega \in R - L$ is real and positive as is $(\alpha - i\beta)X^+$ for $\omega \in L$. $X(\omega)$ either diverges or vanishes at the end points of L, as a power less in magnitude than unity. If X vanishes, the integrals diverge for z at the end point, in such a way that X times the integral is finite. If X diverges, an additional sum-rule condition, that the sum of the integrals vanishes when z is at the end point must be imposed. In either case, $\Delta\sigma'$ is continuous at the end points, and is equal to the value assigned to it by the extrapolation.

(iv) There are an infinite number of sum-rule-like conditions which must be satisfied by the assumed extrapolation if $\Sigma(z)$ and all its derivatives are to be continuous at the end points of L. In our case, these sum rule conditions are not strong and it seems unlikely that conditions of continuity on high derivatives than the first will be useful.

(v) If $\Delta\sigma'$ can be measured at some point or over some small frequency interval, (say by ellipsometry techniques), so that a measured $\Delta\sigma'$ can be used over part of $R - L$, it is best to choose the interval in a region where $|\beta| \gtrsim |\alpha|$. This gives the maximum information. A measurement of $\Delta\sigma'$ at a point where $\beta \ll \alpha$ would give, as a rule, little but confirmation that $\Delta R/R\alpha \simeq \Delta\sigma'$.

In order to illustrate the use of the formula we have applied it to analyse the reflectivity of tungsten as modulated by a surface coverage of hydrogen. This experiment has been briefly discussed elsewhere (Restorff and Drew 1976) and will be the subject of a further report (Restorff 1976). The modulation $\Delta\sigma(\omega)$ has been shown in this case (Fiebelmann 1976) to be given by

$$\Delta\sigma(\omega) = \frac{2i\omega n}{c}\int_{-\infty}^{\infty} [\sigma_H(\omega, x) - \sigma_0(\omega, x)]\, dx \equiv (2i\omega n/c)\sigma_s(\omega) \tag{6}$$

where $\sigma_{H(0)}(\omega, x)$ is the local conductivity of the hydrogen covered (clean) surface at depth x.

In figure 1 we present the data $\Delta R/R$ for the (100) face as well as σ', σ'' for bulk tungsten, which is used to calculate α and β. Further discussion of the data, together with data for other faces will be published elsewhere. Figure 2 shows the resultant $\sigma_s'(\omega)$ based on two

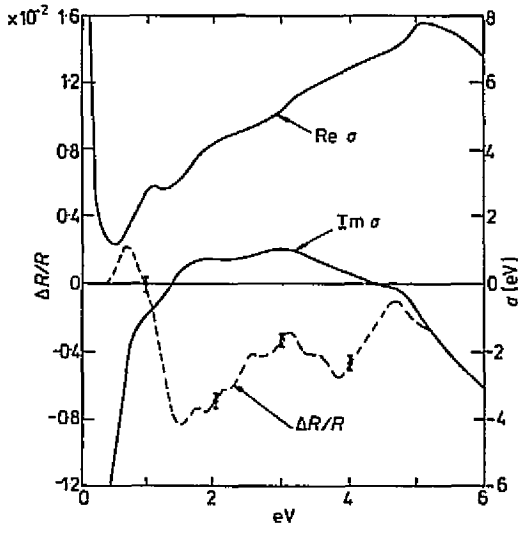

Figure 1. Real and imaginary parts of the conductivity (in frequency units, eV/$\hbar$), for bulk tungsten (solid line). Fractional reflectance for the (100) face of tungsten as modulated by a monolayer coverage of hydrogen. Experimental error is shown.

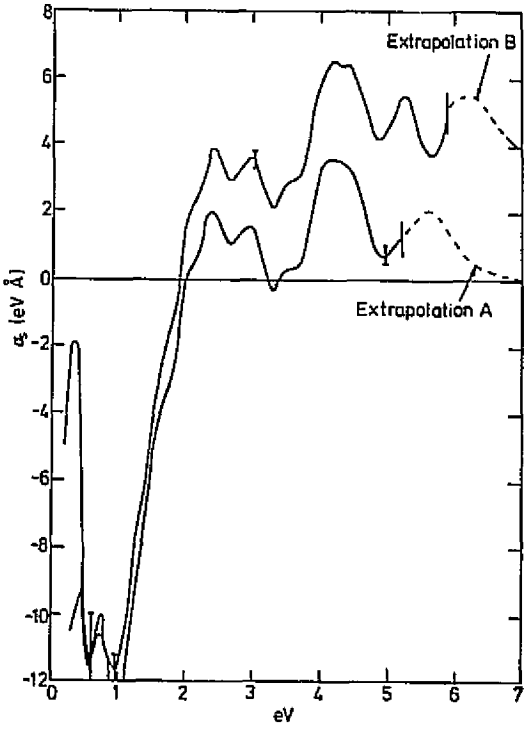

Figure 2. Effective surface conductivity (in frequency units, eV Å/$\hbar$), of hydrogen covered tungsten (defined in the text) as computed from the measured reflectance of figure 1 and two different extrapolations. Error shown arises from experimental error only.

extrapolations. In extrapolation (A), an initial fit using five Lorentz oscillators was made to early data including photon energies only up to 5·2 eV. We note that even here the extrapolation formula (3) was useful, since a preliminary extrapolation taking $\sigma_s' = 0$ above 5·2 eV suggests where the oscillators should be centred. (The least-squares fit has many minimal solutions which it is not easy to distinguish on the basis of goodness of fit.) The oscillator fit above 5·2 eV was then used as the extrapolation in equation (3). We also point out that an earlier oscillator fit (Anderson *et al* 1974), admittedly to somewhat less precise data, replaced the double peak straddling 5 eV by one broad peak. Note also that there is a narrow Lorentz oscillator (not shown) centred at 15 eV with considerable oscillator strength, which is necessary to satisfy the sum rule $\int_0^\infty \sigma_s' \, d\omega = 35 \text{eV}^2$ Å. This isolated oscillator is an unrealistic feature of extrapolation (A).

In extrapolation (B) of figure 2, which is based on more recent data up to 5·9 eV, we have tried to employ what small amount of theory is available at this point. We first note that the new data confirm the splitting at 5 eV and indeed suggest that further structure just above 6 eV will be found.

We do not, however, believe it is meaningful to try to predict structure more than about an electron volt above the end of the experimental data. We choose an extrapolation, cutoff above 20 eV, by $\sigma_s'(\omega) = A/\omega$ + a Lorentz oscillator centered near 6 eV. The Lorentz oscillator represents the peak which we assume exists around 6 or 6·5 eV and A/ω represents a high-frequency average oscillator strength which primarily describes transitions from the extra electrons on the hydrogen. The only reason for supposing that there is a peak near 6 eV is that all extrapolations show that σ_s' is rising at 5·9 eV, and it is difficult to see how this rise could continue to much higher energies.

The reason for choosing the form A/ω is that this seems to be typical of asymptotic forms for transitions between bound states and the continuum. It could be taken as constant without much change in the results. The reason for choosing the cut-off at about 20 eV is as follows.

The wavenumber of the initial and final electron is practically unchanged in the optical transition. The energy of plane waves in the vacuum with wavenumbers of order $1/a_B$ is roughly 20 eV above the probable position of the hydrogen level, some 5–10 volts below the vacuum. (Plane wave states with $k \sim 1/a_B$ in the tungsten have a much lower energy relative to the vacuum.) We have assumed that the wavefunction of the electrons on the hydrogen still have Fourier components with wavenumbers characteristic of the Bohr radius, a_B. The d-electrons on the tungsten are somewhat more compact, and at the surface they are likely to be even more compact than in bulk, according to renormalised atom theory. Thus we would expect some contribution at high energies from shifts induced in the tungsten surface electrons by the absorption of the hydrogen. However, the sum rule for this vanishes and since it is expected to be at somewhat higher frequency, it should have a comparatively small influence on σ_s' in the measured region.

It is not our purpose here to offer a profund analysis of the features to be expected in σ_s'. On the contrary, we suggest that such an analysis is badly needed. What we do hope to have shown is how such an analysis can be of use in pinning down the features of $\Delta\sigma_s'$ over a 'measured' frequency interval.

We have made numerical studies, which will be published elsewhere, of various extrapolation procedures (see also Balzarotti *et al* 1975). In this study, we chose a model $\sigma_s(\omega)$, from which $\Delta R/R$ was calculated. We added noise artificially, and gave it to the analyst to treat as experimental data. (The procedure was 'blind' in the sense that he produced a predicted σ_s without knowing what the model was.) It was found that if the model could be moderately well represented by a few Lorentz oscillators really excellent

results were obtained by extrapolation based on oscillator fits (except below $\frac{1}{2}$ eV). If tails of the type discussed above were used, or other non-Lorentzian shapes employed, the 'base-line' of the data was not so good, although many correct features remained.

Below $\frac{1}{2}$ eV the results were totally unreliable. The reasons for this are that $\Delta R/R$ is small and thus relatively uncertain there, and the bulk σ' is large there. Since the extrapolation gives contributions roughly proportional to the bulk σ' this also introduces large errors.

The example discussed above suffers from the fact that little theory exists on the surface conductivities. We also have under analysis the reflectivity difference between pure Ni or Mo and dilute NiCu and MoRe alloys respectively. Here we expect to be on firmer ground theoretically. One feature in this case is that there will be contributions from extra core electrons in the extrapolation. This contribution can be put in with ease in the present formulation, in contrast to extrapolations of $\Delta R/R$.

Acknowledgments

We acknowledge a grant from the Computer Science Center of the University of Maryland. We wish to thank Professors A Bagchi, T Einstein and R Park for many helpful discussions. We are grateful to Mr M Tokumoto for computational assistance.

References

Anderson J, Rubloff G W, Passler M A and Stiles P J 1974 *Phys. Rev.* B **10** 2401
Bulzarotti A, Colavita E, Gentile S and Rosei R 1975 *Appl. Opt.* **14** 2412
Cardona M 1969 *Modulation Spectroscopy* (New York: Academic Press)
Feibelman P J 1976 *Phys. Rev.* B **14** 762
Mushkilishvili N J 1953 *Singular Integral Equations* (Groningen, Holland: Noordhoff)
Restorff J B 1976 *PhD thesis Univ. of Maryland* and to be published
Restorff J B and Drew H D 1976 *Bull. Am. Phys. Soc.* **21** 305
Seraphin B O and Bottka N 1966 *Phys. Rev.* **145** 628

"MECHANICAL PROPERTIES OF THE ELECTRONIC STRUCTURE OF TRANSITION METAL ALLOYS"

Quarterly Progress Report
for the Period Ending
September 30, 1974

GRANT #NSG-3001

Principal Investigators - Dr. R. J. Arsenault
Dr. H. D. Drew

Submitted to

NASA, Lewis Research Center

UNIVERSITY OF MARYLAND
DEPARTMENT OF PHYSICS AND ASTRONOMY
COLLEGE PARK, MARYLAND
20742

NASA Quarterly Report September 1974

Since initiation of the program our efforts have been directed toward measurements of the differential reflectivity of alloys of molybdenum and elements in the 5d transitional series. The alloy samples have been prepared by evaporation from the bulk in a 10^{-7} torr vacuum to form opaque thin films on quartz substrate. The difference in reflectivity of the alloy and pure molybdenum similarly prepared is continuously recorded as a function of wavelength in the spectral range from 2500 Å to 60,000 Å.

We have measured the differential reflectivity of several samples of MoRe and MoOs in the 5% to 10% concentration range. MoHf has not yet been successfully prepared and MoPt ingots have just been obtained. We have also measured the reflectivity of our pure Mo films over the same spectral range. These results are in good agreement with some values reported in the literature but differ somewhat from the recent results of Veal and Poulikar (Phys. Rev. 1974 to be published). We are presently studying the Kramers-Kronig inversion of our data for the extraction of the complex frequency dependent dielectric constant which the quantity of direct interest. The most interesting result that is already evident in the reflectivity data is the differences in the spectra of the MoRe and MoOs spectra. The corresponding differences in the imaginary part of the dielectric constant will hopefully permit us to learn something about the impurity d levels in the alloy. In particular, the results will test whether the common band model or the virtual level model is more appropriate for this alloy series. Data on MoHf and MoPt is also desirable for this study and we are presently preparing these samples.

Up to now the program has suffered some personnel problems. Dr. Bahl joined the group on May 1 and worked one-half time on the project through the summer. Unfortunately Dr. Bahl had to return to India for a month and is due to return shortly. Another research associate is joining the group in mid October and will be taking over the research on a full-time basis.

Quarterly Progress Report

December 20, 1974

MECHANICAL PROPERTIES AND THE ELECTRONIC STRUCTURE OF TRANSITION METAL ALLOYS

Grant #NSG-3001

Submitted to

National Aeronautics and Space Administration

LEWIS RESEARCH CENTER

Cleveland, Ohio

by

R. J. Arsenault
H. D. Drew
University of Maryland
College Park, Maryland

During the third quarter of the first year of this program we have continued our differential reflectivity measurements on the Mo based alloys and worked on the Kramers-Kronig analysis of the optical data. Dr. Bahl has returned from India and we are now making rapid progress toward the completion of the measurement and anaylsis of the optical properties of the dilute alloys.

In an effort to improve the quality of our evaporated samples we have tested samples deposited on a quartz substrate heated to 600° C. This procedure is expected to produce a better film because of the outgassing of trapped gases and because of the higher mobility of the deposited metal atom at the elevated substrate temperature. Having seen a noticeable improvement in the reflectivity of pure Mo for samples prepared this way we are now preparing all our films on heated substrates. We have completed the low concentration measurements of MoRe and MoOs and we are now studying MoPt films.

These optical studies are at the critical stage where interesting information concerning the electronic structure of the alloys is becoming available. In Fig. 1 and 2 we show the optical data and the preliminary results for the imaginary part of the dielectric constant, ε_2, derived from a Kramers-Kronig analysis of the optical data. $\Delta\varepsilon_2 = \varepsilon_2^A - \varepsilon_2^P$ is plotted in Fig. 2 v.s. photon energy in electron volts. These data show the following main features: 1. at low frequencies the increased electronic scattering in the alloy produces a positive $\Delta\varepsilon_2$ from the Drude response of the S "band" electrons near the Fermi level; 2. above about 1 eV the $\Delta\varepsilon_2$ becomes negative and has the general shape of ε_2 of pure Mo. This feature can be interpreted in terms of a reduction in the number of electrons in the Mo "d bands". This interpretation raises the question of the location of the impurity d electrons. If they go in as relatively localized states (in space and in energy) we would expect

them to lie near the Fermi energy and be partially masked by the Drude response.

We are refining our analysis of the optical data in order to test these hypotheses. The MoPt optical data and the resistivity data which we are also measuring for all these alloys, will be very helpful in the analysis. We expect significant results from these studies in the very near future.

MECHANICAL PROPERTIES OF THE ELECTRONIC STRUCTURE OF TRANSITION METAL ALLOYS

Quarterly Progress Report
for the Period Ending
September 30, 1975

GRANT #NSG-3001

Principal Investigators - Dr. R. J. Arsenault
Dr. H. D. Drew

Submitted to

NASA, Lewis Research Center

UNIVERSITY OF MARYLAND
DEPARTMENT OF PHYSICS AND ASTRONOMY
COLLEGE PARK, MARYLAND
20742

Summary of Year's Research

We have completed the work on alloy films prepared by evaporating bulk alloys. The case of MoRe alloys has been carefully examined.[2] The results of optical and electrical measurements indicate that the Re d electrons lie in localized states at the Re site and located about 1 eV below the Fermi level. In addition, it appears that t d density of states at the Fermi level decreases upon alloying with Re. These results can be qualitatively understood in terms of the Anderson extra orbital model as it has been applied to problems in the theory of chemisorption.[1] In this theory the impurity density of states can be nonzero over the whole range of the host (Mo) d bands and peaks are expected where the host density of states is low. The Re d states appear to be lying near the minimum of the Mo density of states near the Fermi level. A short paper on this work has been submitted for publication in the Journal of the Less Common Metals and a preprint is attached to this report in the Appendix.

Evaporating films from bulk alloy samples proved to be only marginally successful. Although it enabled us to complete a study of MoRe alloys, we were unable to do a careful study of the concentration dependence of MoRe and it proved totally unsatisfactory for MoOs and MoPt alloys. For these last two, the evaporation rates of the two constituents differed too greatly to permit making useful films. Also, difficulties were encountered in ascertaining sample compositions reliably and inexpensively.

Because of these difficulties we have installed a second e-gun source in our evaporator so that we now have a 6 kW source in addition to the original 2 kW source. With this modification along with other improvements in the evaporator we can now prepare films of predetermined composition by co-evaporation of the constituent metals onto a preheated substrate. The evaporator configuration is shown in Fig. 1. With the larger e-gun source higher evaporation rates are possible which has produced higher quality films. The pure Mo films are

now found to have a higher residual resistance ratio (∿ 10) and a reflectivity that is closer to the best results reported for bulk films in high vacuum.[3] (Fig. 2) Examination of these films by x-ray and electron diffraction show that they are polycrystalline with crystallite size much greater than 500 Å. After installing the e-gun and rebuilding the evaporator we have calibrated the film thickness monitor and determined the optimum conditions for evaporating films. With this improvement we have solved many of the difficult problems associated with preparing high quality alloy samples of known composition for the optical studies.

We are presently studying MoOs alloys as the logical step following our work on the MoRe system. Preliminary optical data for a MoOs film is shown in Fig. 3. The strong peak at about 3 eV is indicative of a shift of the solute d levels toward lower energies for Os as compared with Re (where the peak is around 1 eV). Preliminary resistivity measurements for the MoOs films give $\Delta\rho/c$ = 1.9 μΩ-cm/at. This value is somewhat lower than for MoRe films for which we have measured $\Delta\rho/c$ = 2.2 μΩ-cm/at.%. This result is also consistent with the above interpretation. We are presently repeating these studies for different Os concentrations and performing further analysis of these data.

Considerable interest has developed among the theorists in our Solid State Physics group on the question of the effects of the electronic structure of these alloys on their hardness properties. Part of this interest derives from the close relation between the theories of these alloys and the theories of chemisorption for gas atoms on W and Mo.[1] As we learn more about the electronic structure of these alloys, our effort to explain the dependence of the hardness on the number of d electrons in the alloy may be assisted by their participation.

We have almost developed a computer program to determine the Peierls' stress from an anisotropic interatomic potential. Hopefully the inserting of a solute atom of a different atomic potential will not be too difficult or too time consuming.

From our classical solid solution modeling we have been able to determine the effect of a size difference (strain) on the yield stress at 0 K (Fig. 4). The value of τ_p (Peierls' stress) chosen for Mo was 60 kg/mm^2. The solid line

represents the yield stress as a function of size differences for a solute concentration of 1%, whereas, the dashed line represents a solute concentration of 10%. The arrows with the chemical symbols on top indicate the strain (size difference) of the various solute additions. In the case of Os there is a difference depending upon the reference employed.[4,5]

If a 1% solid solution is considered then increasing the size difference results in a decrease in strength, i.e., solid solution weakening, which means that Hf should produce a larger degree of solid solution weakening than Re. This is in direct disagreement with the experimental results,[4] but these results were expected, however the modulus effect has yet to be considered. If a 10% solid solution is considered then the solid solution weakening occurs for strains less than 0.06, and strengthening occurs for strains greater than 0.06. Again there is no general agreement between the computer simulation results and the experimental results at 0 K.

We have also determined the strengthening as a function of temperature for two strains and two compositions (Fig. 5,6). This higher temperature region is of greater interest, for the computer simulation results predict strengthening for both values of strain and composition, which is in agreement with the experimental results. Again, additional compositions will have to be examined along with the modulus difference effect.

REFERENCES

1. J. R. Schrieffer, J. of Vacuum Science and Technology 9, 561 (1972).
2. S. K. Bahl and H. D. Drew, to be published and appendix of this report.
3. B. W. Veal and A. P. Paulikas, Phys. Rev. B10, 1280 (1974).
4. J. R. Stephens and W. R. Witzke, J. of Less Common Metals 29, 371 (1972).
5. G. V. Raynor, Phil. Mag. 31, 1099 (1975).
6. D. M. Newns, Phys. Rev. 178, 1123 (1969).

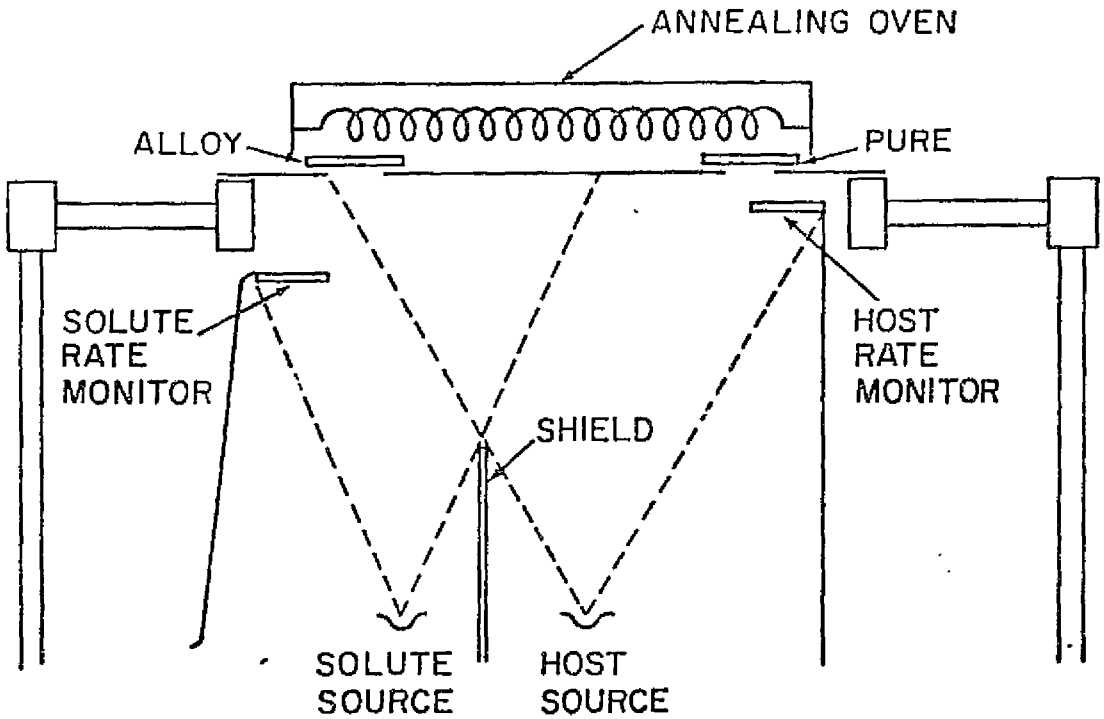

Fig. 1

Evaporator geometry for simultaneous preparation of pure and alloy films of predetermined composition.

Reflectivity of our pure Mo films compared with the best results reported for bulk Mo in high vacuum. The agreement is seen to be excellent below 3 eV and beginning to deviate substantially only at high photon energies. These results are better than any previously reported results on films.

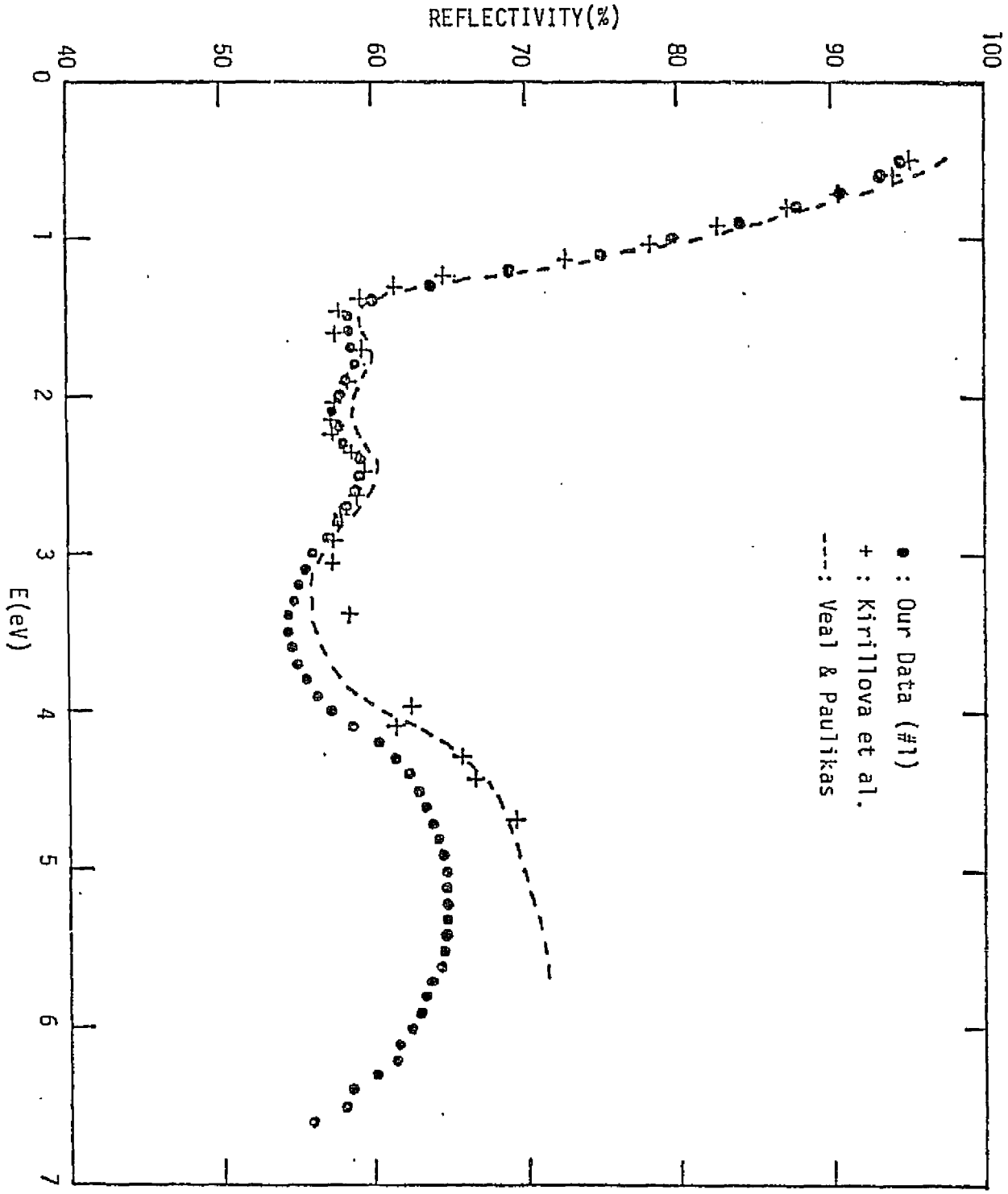

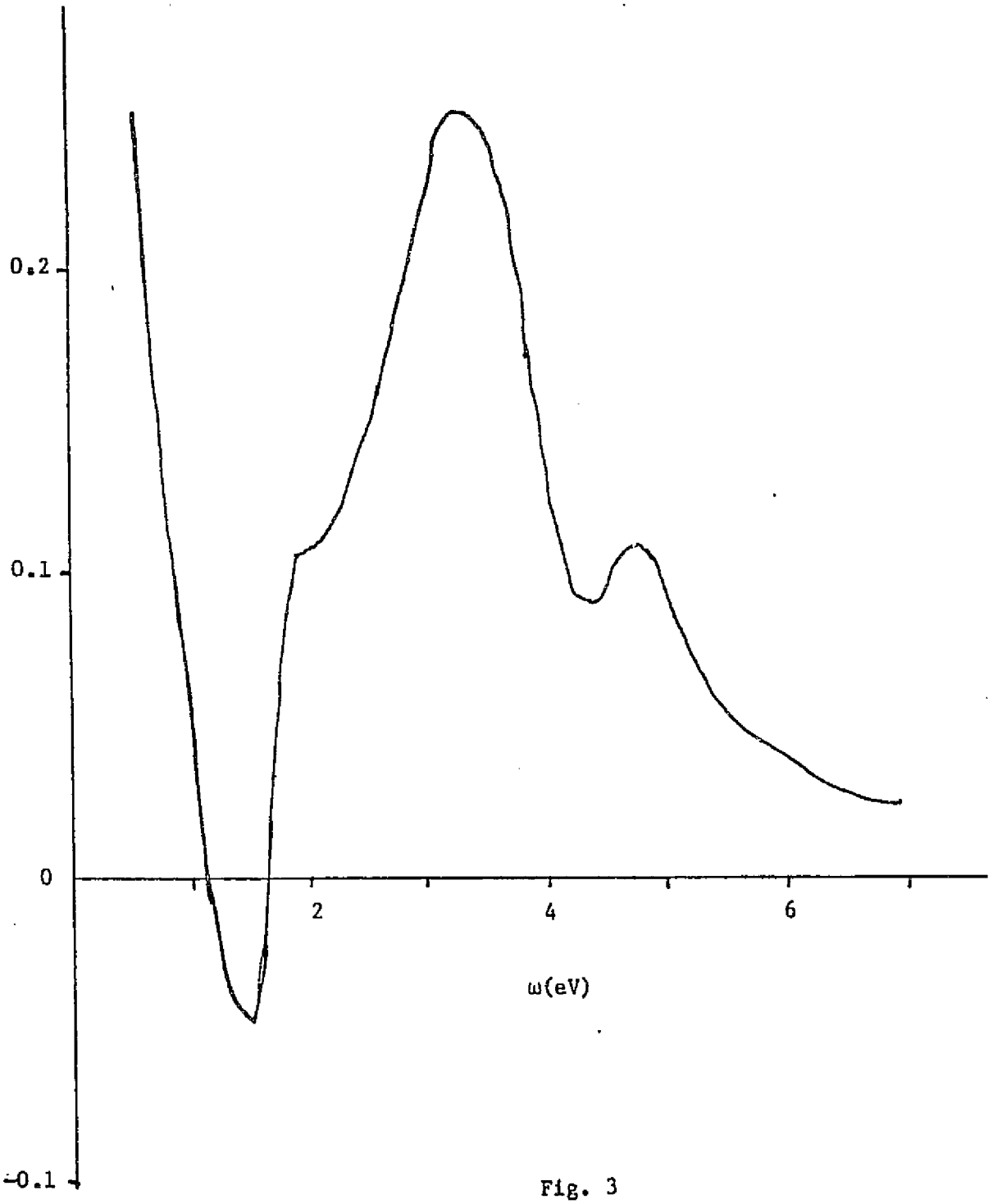

Fig. 3

Difference in optical conductivity for a 2 at.% Mo Os alloy

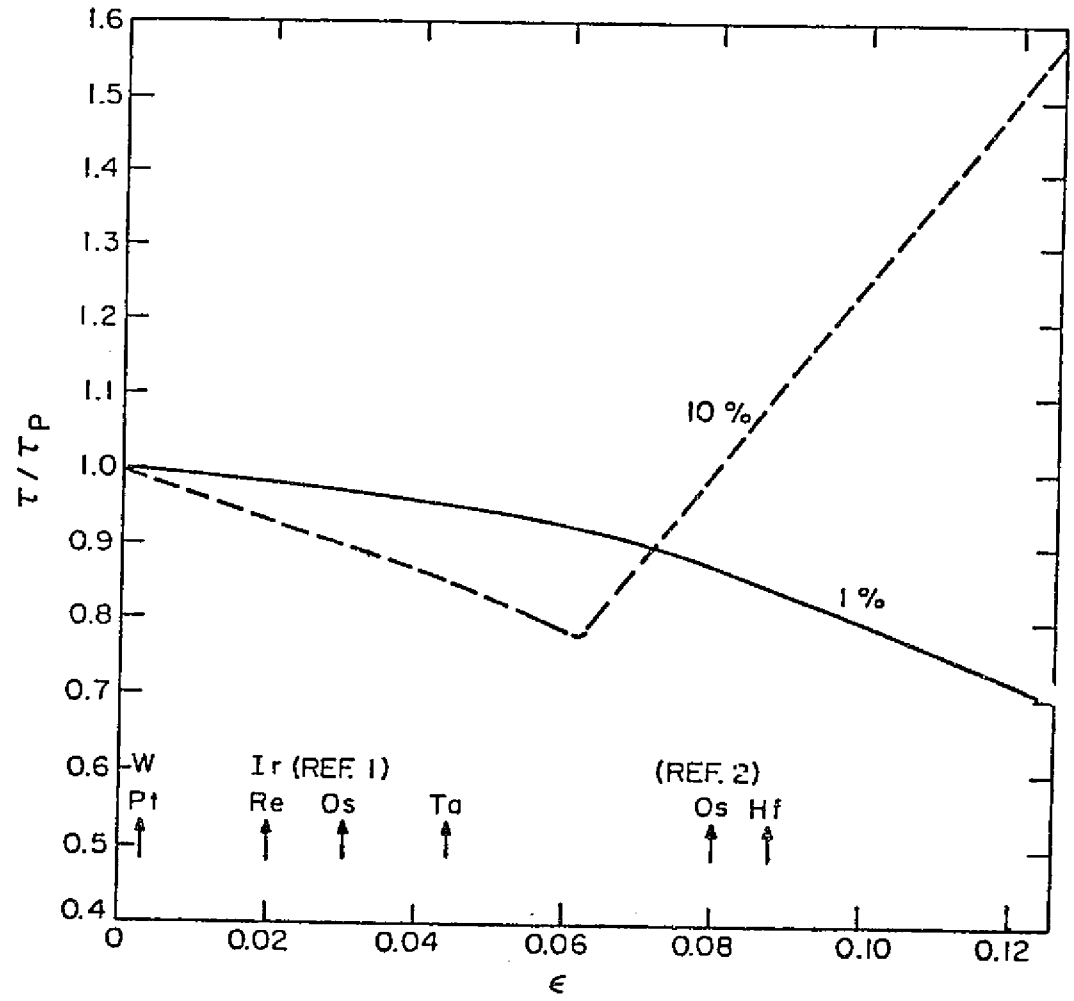

Fig. 4. The variation of yield stress due to differences in strain at 0 K.

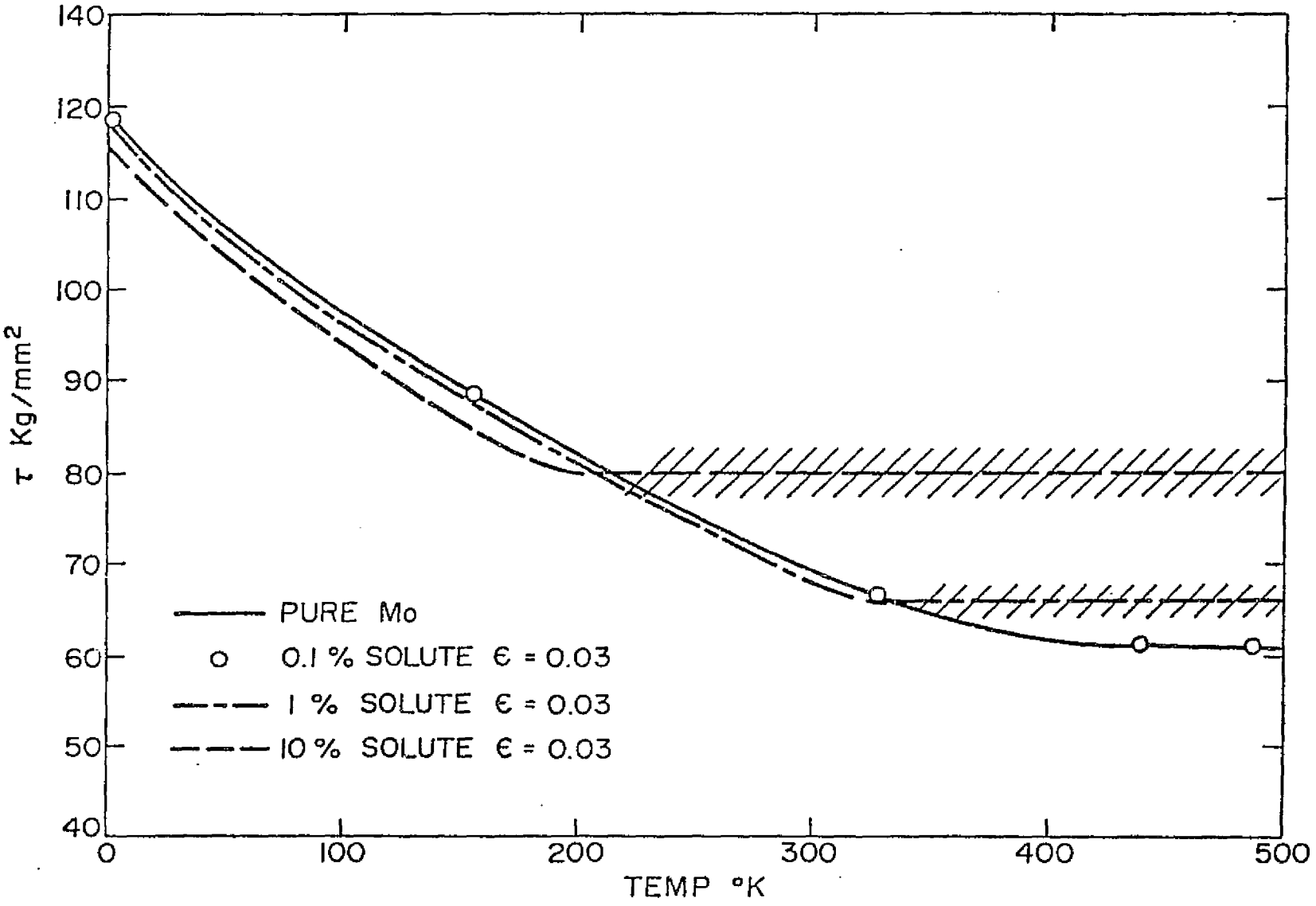

Fig. 5. The yield stress as a function of temperature for two different concentrations for a strain of 0.08.

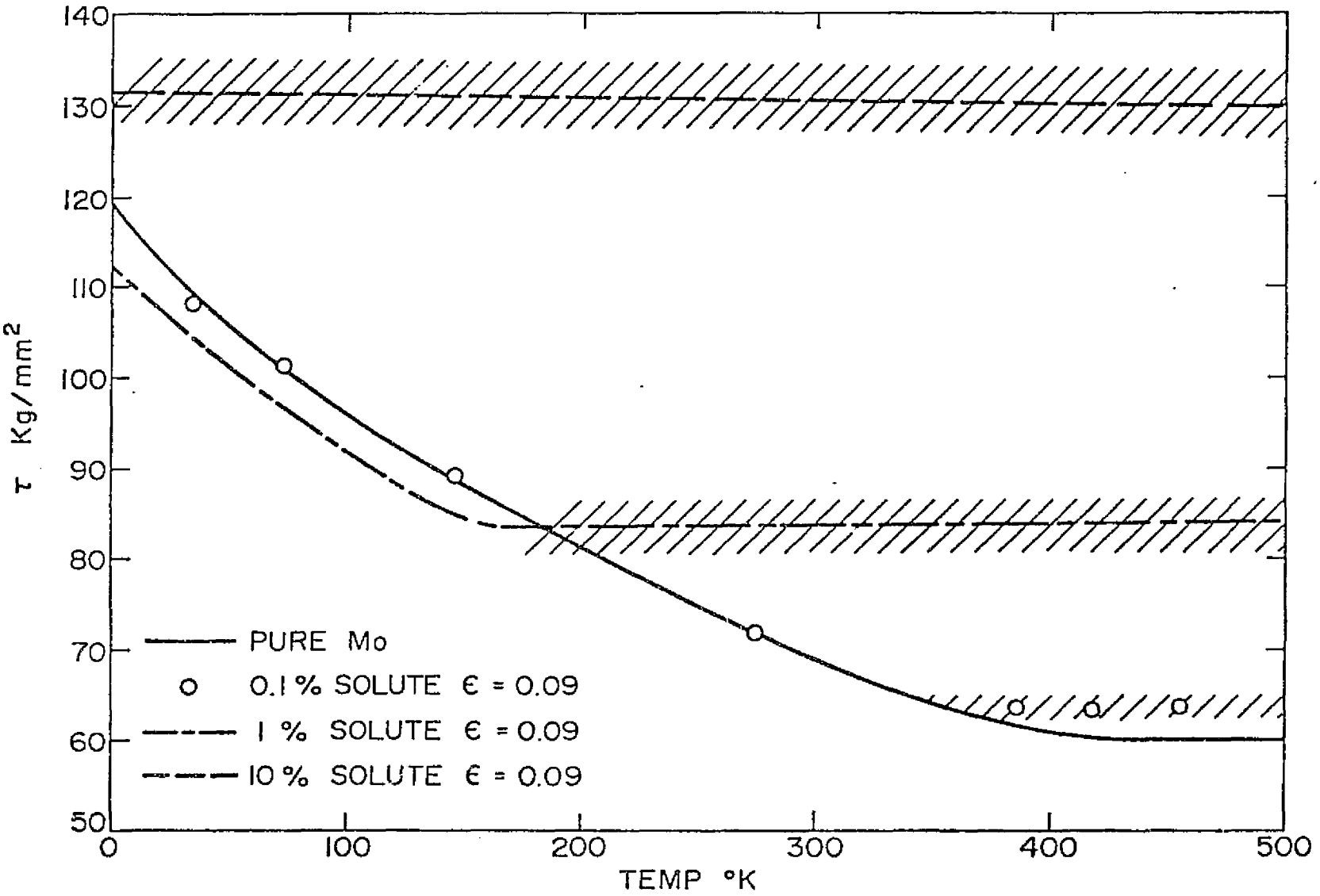

Fig. 6. The yield stress as a function of temperature for two different concentrations for a strain of 0.09.

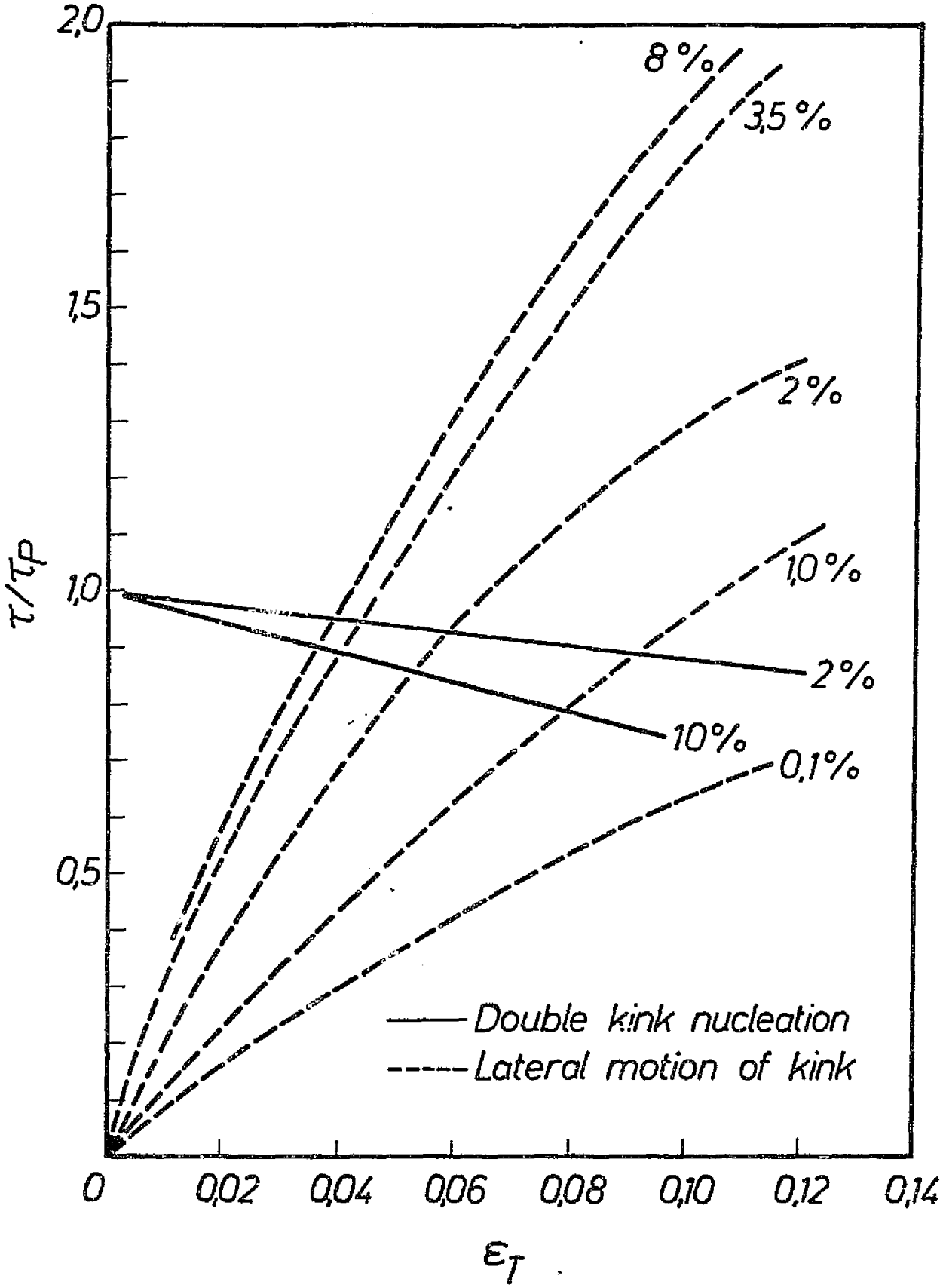
2,0
1,5
1,0
0,5
τ/τp
8 %
3,5 %
2 %
1,0 %
2 %
10 %
0,1 %
Double kink nucleation
Lateral motion of kink
0
0,02
0,04
0,06
0,08
0,10
0,12
0,14
εT

Fig. 7

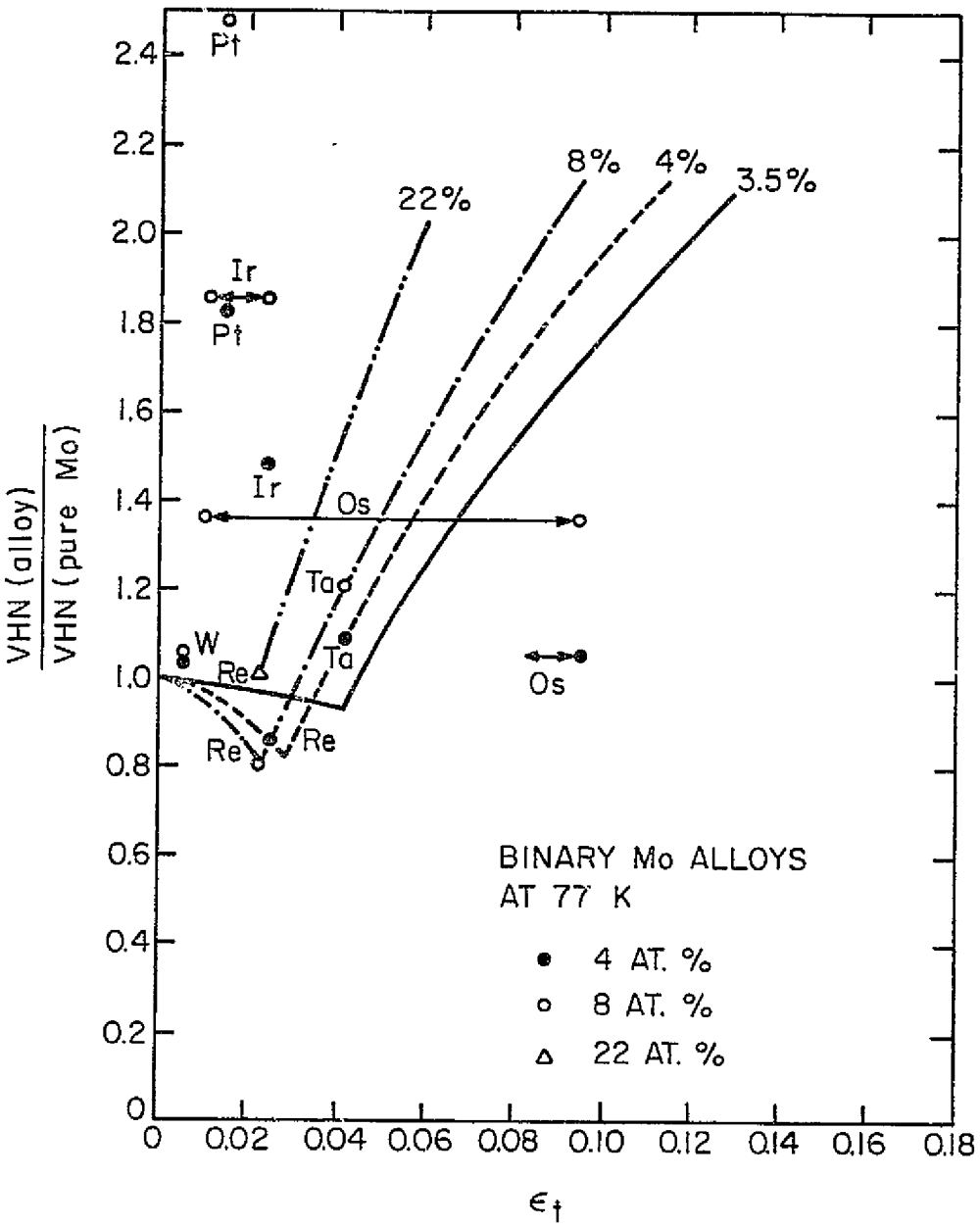

Fig. 8